Nakamura Y, Matsuo J, Miyamoto N, Ojima A, Ando K, Kanda Y, Sawada K, Sugiyama A, **Sekino Y**	Assessment of testing methods for drug-induced repolarization delay and arrhythmias in an iPS cell-derived cardiomyocyte sheet: multi-site validation study.	***J Pharmacol Sci***	124(4)	494-501	2014
Ishikawa M, Shiota J, Ishibashi Y, Hakamata T, Shoji S, Fukuchi M, Tsuda M, Shirao T, **Sekino Y**. Baraban JM, Tabuchi A	Cellular localization and dendritic function of rat isoforms of the SRF coactivator MKL1 in cortical neurons.	***Neuroreport***	25(8)	585-92	2014
Takayama K., Nagamoto Y., Mimura N., Tashiro K., Sakurai F., Tachibana M., Hayakawa T., **Kawabata K.**, Mizuguchi H.	Long-Term Self-Renewal of Human ES/iPS-Derived Hepatoblast-like Cells on Human Laminin 111-Coated Dishes.	***Stem Cell Reports***	1	322-335	2013
Takayama K., **Kawabata K.**, Inamura M., Ohashi K., Nagamoto Y., Okuno H., Yamaguchi T., Tashiro K., Sakurai F., Hayakawa T., Furue-Kusuda M., Mizuguchi H.	CCAAT/enhancer binding protein-mediated regulation of TGFβ receptor 2 expression determine the hepatoblast fate decision.	***Development***	141	91-100	2014
Yamaguchi T., Tashiro K., Tanaka S., Katayama S., Ishida W., Fukuda K., Fukushima A., Araki R., Abe M., Mizuguchi H., **Kawabata K**.	Two-step differentiation of mast cells from induced pluripotent stem cells.	***Stem Cells Dev.***	22	726-734	2013
Ishikawa M., Shiota J., Ishibashi Y., Hakamata T., Shoji S., Fukuchi M., Tsuda M., Shirao T., **Sekino Y.**, Ohtsuka T., Baraban J.M., Tabuchi A.	Identification, expression and characterization of rat isoforms of the SRF coactivator MKL1.	***FEBS Open Bio.***	3	387-93	2013

Takahashi K., Ishii-Nozawa R., Takeuchi K., Nakazawa K., **Sekino Y.**, Sato K.	Niflumic acid activates additional currents of the human glial L-glutamate transporter EAAT1 in a substrate-dependent manner.	***Biol Pharm Bull***	36(12)	1996-2004	2013
Oguchi-Katayama A., Monma A., **Sekino Y.**, Moriguchi T., Sato K.	Comparative gene expression analysis of the amygdalae of juvenile rats exposed to valproic acid at prenatal and postnatal stages.	***J Toxicol Sci***	38(3)	381-402	2013
Yamada S., Kotake Y., **Sekino Y.**, Kanda Y.	AMP-activated protein kinase-mediated glucose transport as a novel target of tributyltin in human embryonic carcinoma cells.	***Metallomics***	5	484-91	2013
山口朋子、**川端健二**	iPS細胞由来マスト細胞を用いた難治性疾患の新規治療薬開発へ向けて	***Biophilia電子版***	2	21-25	2013
Tashiro K., Omori M., **Kawabata K.**, Hirata N., Yamaguchi T., Sakurai F., Takaki S., Mizuguchi H.	Inhibition of Lnk in Mouse Induced Pluripotent Stem Cells Promotes Hematopoietic Cell Generation.	***Stem Cells Dev.***	21	3381-3390	2012
Tashiro K., **Kawabata K.**, Omori M., Yamaguchi T., Sakurai F., Katayama K., Hayakawa H., Mizuguchi H.	Promotion of hematopoietic differentiation from mouse induced pluripotent stem cells by transient HoxB4 transduction.	***Stem Cell Res.***	8	300-311	2012
Takayama K., **Kawabata K.**, Nagamoto Y., Kishimoto K., Tashiro K., Sakurai F., Tachibana M., Kanda K., Hayakawa T., Furue MK., Mizuguchi H.	3D spheroid culture of hESC/hiPSC-derived hepatocyte-like cells for drug toxicity testing.	***Biomaterials***	34	1781-1789	2013

Takayama K., Inamura M., **Kawabata K.**, Sugawara M., Kikuchi K., Higuchi M., Nagamoto Y., Watanabe H., Tashiro K., Sakurai F., Hayakawa T., Furue MK., Mizuguchi H.	Generation of metabolically functioning hepatocytes from human pluripotent stem cells by FOXA2 and HNF1α transduction.	***J. Hepatol.***	57	628-636	2012
Nagamoto Y., Tashiro K., Takayama K., Ohashi K., **Kawabata K.**, Sakurai F., Tachibana M., Hayakawa T., Furue MK., Mizuguchi H.	The promotion of hepatic maturation of human pluripotent stem cells in 3D co-culture using type I collagen and Swiss 3T3 cell sheets.	***Biomaterials***	33	4526-4534	2012
Takayama K., Inamura M., **Kawabata K.**, Katayama K., Higuchi M., Tashiro K., Nonaka A., Sakurai F., Hayakawa T., Furue MK., Mizuguchi H.	Efficient generation of functional hepatocytes from human embryonic stem cells and induced pluripotent stem cells by HNF4α transduction.	***Mol. Ther.***	20	127-137	2012
Takaki J., Fujimori K., Miura M., Suzuki T., **Sekino, Y.**, Sato, K.	L-glutamate released from activated microglia downregulates astrocytic L-glutamate transporter expression in neuroinflammation: the 'collusion' hypothesis for increased extracellular L-glutamate concentration in neuroinflammation.	***J. Neuro-inflammation***	9	275	2012
Sato K., Kuriwaki J., Takahashi K., Saito Y., Oka J., Otani Y., Sha Y., Nakazawa K., **Sekino Y.**, Ohwada T.	Discovery of a tamoxifen-related compound that suppresses glial L-glutamate transport activity without Interaction with estrogen receptors.	***ACS Chem Neurosci***	3 (2)	105-113	2012
Kawabata K., Takayama K., Nagamoto Y., Saldon MM., Higuchi M., Mizuguchi H.	Endodermal and hepatic differentiation from human embryonic stem cells and human induced pluripotent stem cells.	***J. Stem Cell Res. Ther.***	S10	002	2012

Kawabata K., Inamura M., Mizuguchi H.	Efficient hepatic differentiation from human iPS cells by gene transfer.	***Methods Mol. Biol.***	826	115-124	2012
水口裕之、高山和雄、長基康人、**川端健二**	ヒトiPS細胞から肝細胞への分化誘導の現状と創薬応用	医薬品医療機器レギュラトリーサイエンス	43	982-987	2012
高山和雄、**川端健二**、水口裕之	ヒトES/iPS細胞から肝細胞への高効率分化誘導法の開発とその創薬応用	最新医学	68	141-144	2013
川端健二、高山和雄、水口裕之	ヒトiPS細胞由来分化誘導肝細胞を用いた薬物毒性評価系の開発	バイオインダストリー	30	19-24	2013

Prediction of interindividual differences in hepatic functions and drug sensitivity by using human iPS-derived hepatocytes

Kazuo Takayama[a,b,c], Yuta Morisaki[a], Shuichi Kuno[a], Yasuhito Nagamoto[a,c], Kazuo Harada[d], Norihisa Furukawa[a], Manami Ohtaka[e], Ken Nishimura[f], Kazuo Imagawa[a,c,g], Fuminori Sakurai[a,h], Masashi Tachibana[a], Ryo Sumazaki[g], Emiko Noguchi[i], Mahito Nakanishi[e], Kazumasa Hirata[d], Kenji Kawabata[j,k], and Hiroyuki Mizuguchi[a,b,c,l,1]

[a]Laboratory of Biochemistry and Molecular Biology; [b]iPS Cell-based Research Project on Hepatic Toxicity and Metabolism, [d]Laboratory of Applied Environmental Biology, [h]Laboratory of Regulatory Sciences for Oligonucleotide Therapeutics, Clinical Drug Development Project, and [k]Laboratory of Biomedical Innovation, Graduate School of Pharmaceutical Sciences, Osaka University, Osaka 565-0871, Japan; [c]Laboratory of Hepatocyte Regulation, and [j]Laboratory of Stem Cell Regulation, National Institute of Biomedical Innovation, Osaka 567-0085, Japan; [e]Research Center for Stem Cell Engineering, National Institute of Advanced Industrial Science and Technology, Ibaraki 305-8562, Japan; [f]Laboratory of Gene Regulation, [g]Department of Child Health, and [i]Department of Medical Genetics, Faculty of Medicine, University of Tsukuba, Ibaraki 305-8575, Japan; and [l]The Center for Advanced Medical Engineering and Informatics, Osaka University, Osaka 565-0871, Japan

Edited by Shinya Yamanaka, Kyoto University, Kyoto, Japan, and approved October 17, 2014 (received for review July 16, 2014)

Interindividual differences in hepatic metabolism, which are mainly due to genetic polymorphism in its gene, have a large influence on individual drug efficacy and adverse reaction. Hepatocyte-like cells (HLCs) differentiated from human induced pluripotent stem (iPS) cells have the potential to predict interindividual differences in drug metabolism capacity and drug response. However, it remains uncertain whether human iPSC-derived HLCs can reproduce the interindividual difference in hepatic metabolism and drug response. We found that cytochrome P450 (CYP) metabolism capacity and drug responsiveness of the primary human hepatocytes (PHH)-iPS-HLCs were highly correlated with those of PHHs, suggesting that the PHH-iPS-HLCs retained donor-specific CYP metabolism capacity and drug responsiveness. We also demonstrated that the interindividual differences, which are due to the diversity of individual SNPs in the CYP gene, could also be reproduced in PHH-iPS-HLCs. We succeeded in establishing, to our knowledge, the first PHH-iPS-HLC panel that reflects the interindividual differences of hepatic drug-metabolizing capacity and drug responsiveness.

human iPS cells | hepatocyte | CYP2D6 | personalized drug therapy | SNP

Drug-induced liver injury (DILI) is a leading cause of the withdrawal of drugs from the market. Human induced pluripotent stem cell (iPSC)-derived hepatocyte-like cells (HLCs) are expected to be useful for the prediction of DILI in the early phase of drug development. Many groups, including our own, have reported that the human iPS-HLCs have the ability to metabolize drugs, and thus these cells could be used to detect the cytotoxicity of drugs that are known to cause DILI (1, 2). However, to accurately predict DILI, it will be necessary to establish a panel of human iPS-HLCs that better represents the genetic variation of the human population because there are large interindividual differences in the drug metabolism capacity and drug responsiveness of hepatocytes (3). However, it remains unclear whether the drug metabolism capacity and drug responsiveness of human iPS-HLCs could reflect those of donor parental primary human hepatocytes (PHHs). To address this issue, we generated the HLCs differentiated from human iPSCs which had been established from PHHs (PHH-iPS-HLCs). Then, we compared the drug metabolism capacity and drug responsiveness of PHH-iPS-HLCs with those of their parental PHHs, which are genetically identical to the PHH-iPS-HLCs.

Interindividual differences of cytochrome P450 (CYP) metabolism capacity are closely related to genetic polymorphisms, especially single nucleotide polymorphisms (SNPs), in CYP genes (4). Among the various CYPs expressed in the liver, CYP2D6 is responsible for the metabolism of approximately a quarter of commercially used drugs and has the largest phenotypic variability, largely due to SNPs (5). It is known that certain alleles result in the poor metabolizer phenotype due to a decrease of CYP2D6 metabolism. Therefore, the appropriate dosage for drugs that are metabolized by CYP2D6, such as tamoxifen, varies widely among individuals (6). Indeed, in the 1980s, polymorphism in CYP2D6 appears to have contributed to the withdrawal of CYP2D6-metabolized drugs such as perhexiline from the market in many countries (7). If we could establish a panel of HLCs that better represents the diversity of genetic polymorphisms in the human population, it might be possible to determine the appropriate dosage of a drug for a particular individual. However, it is not known whether the drug metabolism capacity and drug responsiveness of HLCs reflect the genetic diversity, including SNPs, in CYP genes. Therefore, in this study we generated HLCs from several PHHs that have various SNPs on CYP2D6 and then compared the CYP2D6 metabolism capacity and responses to CYP2D6-metabolized drugs between the PHH-iPS-HLCs and parental PHHs.

Significance

We found that individual cytochrome P450 (CYP) metabolism capacity and drug sensitivity could be predicted by examining them in the primary human hepatocytes–human induced pluripotent stem cells–hepatocyte-like cells (PHH-iPS-HLCs). We also confirmed that interindividual differences of CYP metabolism capacity and drug responsiveness that are due to the diversity of individual single nucleotide polymorphisms in the CYP gene could also be reproduced in the PHH-iPS-HLCs. These findings suggest that interindividual differences in drug metabolism capacity and drug response could be predicted by using HLCs differentiated from human iPS cells. We believe that iPS-HLCs would be a powerful technology not only for accurate and efficient drug development, but also for personalized drug therapy.

Author contributions: K.T. and H.M. designed research; K.T., Y.M., and S.K. performed research; K.T., Y.M., Kazuo Harada, M.O., K.N., K.I., M.N., and Kazumasa Hirata contributed new reagents/analytic tools; K.T., Y.N., N.F., F.S., M.T., R.S., E.N., K.K., and H.M. analyzed data; and K.T. and H.M. wrote the paper.

The authors declare no conflict of interest.

This article is a PNAS Direct Submission.

Data deposition: The DNA microarray data reported in this paper have been deposited in the Gene Expression Omnibus (GEO) database, www.ncbi.nlm.nih.gov/geo (accession no. GSE61287).

[1]To whom correspondence should be addressed. Email: mizuguch@phs.osaka-u.ac.jp.

This article contains supporting information online at www.pnas.org/lookup/suppl/doi:10.1073/pnas.1413481111/-/DCSupplemental.

To this end, PHHs were reprogrammed into human iPSCs and then differentiated into the HLCs. To examine whether the HLCs could reproduce the characteristics of donor PHHs, we first compared the CYP metabolism capacity and response to a hepatotoxic drug between PHHs and genetically identical PHH-iPS-HLCs (12 donors were used in this study). Next, analyses of hepatic functions, including comparisons of the gene expression of liver-specific genes and CYPs, were performed to examine whether the hepatic characteristics of PHHs were reproduced in the HLCs. To the best of our knowledge, this is the first study to compare the functions between iPSC-derived cells from various donors and their parental cells with identical genetic backgrounds. Finally, we examined whether the PHH-iPS-HLCs exhibited a capacity for drug metabolism and drug responsiveness that reflect the genetic diversity such as SNPs on CYP genes.

Results

Reprogramming of PHHs to Human iPSCs. To examine whether the HLCs could reproduce interindividual differences in liver functions, we first tried to generate human iPSCs from the PHHs of 12 donors. PHHs were transduced with a Yamanaka 4 factor-expressing SeV (SeVdp-iPS) vector (*SI Appendix*, Fig. S1*A*) in the presence of SB431542, PD0325901, and a rock inhibitor, which could promote the somatic reprogramming (8). The reprogramming procedure is shown in *SI Appendix*, Fig. S1*B*. The human iPSCs generated from PHHs (PHH-iPSCs) were positive for alkaline phosphatase (*SI Appendix*, Fig. S1*B*, *Right*), NANOG, OCT4, SSEA4, SOX2, Tra1-81, and KLF4 (Fig. 1*A*). The gene expression levels of the pluripotent markers (*OCT3/4*, *SOX2*, and *NANOG*) in the PHH-iPSCs were approximately equal to those in human embryonic stem cells (ESCs) (*SI Appendix*, Fig. S1*C*, *Left*). The gene expression levels of the hepatic markers [*albumin (ALB)*, *CYP3A4*, and *αAT*] in the PHH-iPSCs were significantly lower than those in the parental PHHs (*SI Appendix*, Fig. S1*C*, *Right*). We also confirmed that the PHH-iPSCs have the ability to differentiate into the three embryonic germ layers in vitro by embryoid body formation and in vivo by teratoma formation (*SI Appendix*, Fig. S2 *A* and *B*, respectively). To verify that the PHH-iPSCs originated from PHHs, short tandem repeat analysis was performed in the PHH-iPSCs and parental PHHs (*SI Appendix*, Fig. S2*C*). The results showed that the PHH-iPSCs were indeed originated from PHHs. Taken together, these results indicated that the generation of human iPSCs from PHHs was successfully performed. It is known that a transient epigenetic memory of the original cells is retained in early-passage iPSCs, but not in late-passage iPSCs (9). To examine whether the hepatic differentiation capacity of PHH-iPSCs depends on their passage number, PHH-iPSCs having various passage numbers were differentiated into the hepatic lineage (Fig. 1*B*). The *tyrosine aminotransferase* (*TAT*) expression levels and albumin (ALB) secretion levels in early passage PHH-iPS-HLCs (fewer than 10 passages) were higher than those of late passage PHH-iPS-HLCs (more than 14 passages). These results suggest that the hepatic differentiation tendency is maintained in early passage PHH-iPSCs, but not in late passage PHH-iPSCs. In addition, the hepatic functions of late passage PHH-iPS-HLCs were similar to those in the HLCs derived from late passage non–PHH-derived iPS cells (such as dermal cells, blood cells, and Human Umbilical Vein Endothelial Cells (HUVEC)-derived iPS cells) (*SI Appendix*, Fig. S3). Therefore, PHH-iPSCs, which were passaged more than 20 times, were used in our study to avoid any potential effect of transient epigenetic memory retained in parental PHHs on hepatic functions.

HLCs Were Differentiated from PHH-iPSCs Independent of Their Differentiation Tendency. To compare the hepatic characteristics among the PHH-iPS-HLCs that were generated from PHHs of

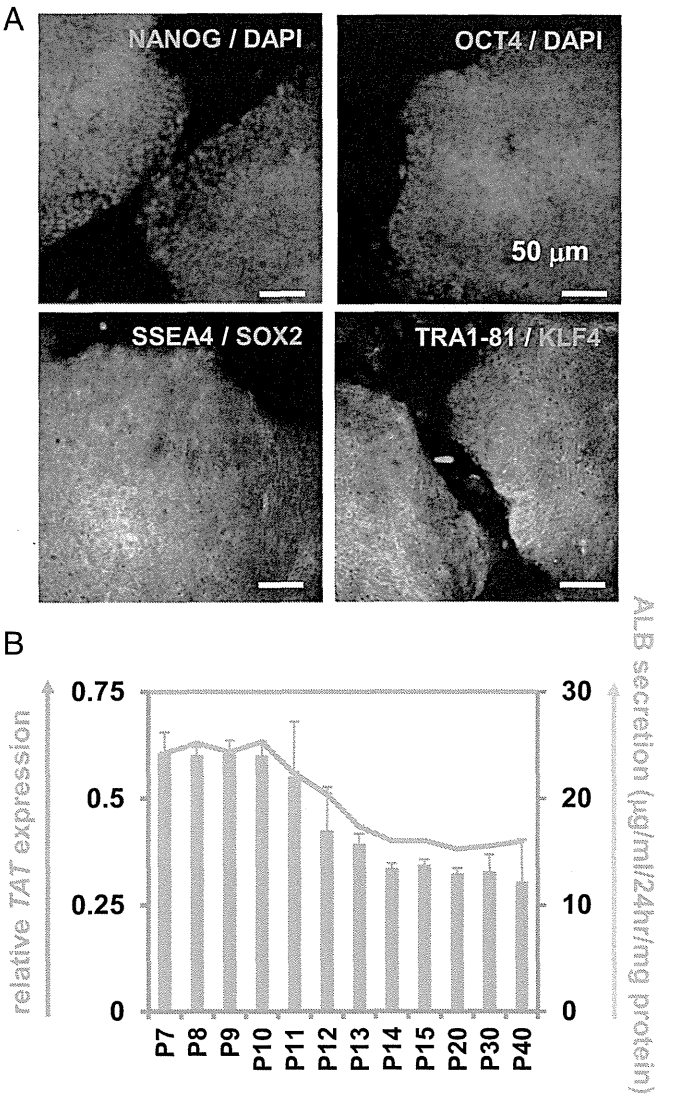

Fig. 1. Establishment and characterization of human iPSCs generated from PHHs. (*A*) The PHH-iPSCs were subjected to immunostaining with anti-NANOG (red), OCT4 (red), SSEA4 (green), SOX2 (red), TRA1-81 (green), and KLF4 (red) antibodies. Nuclei were counterstained with DAPI (blue) (*Upper*). (*B*) The *TAT* expression and ALB secretion levels in the PHH-iPS-HLCs (P7–P40) were examined. On the *y* axis, the gene expression level of *TAT* in PHHs was taken as 1.0.

the 12 donors, all of the PHH-iPSCs were differentiated into the HLCs as described in Fig. 2*A*. However, the differences in hepatic function among PHH-iPS-HLCs could not be properly compared because there were large inter-PHH-iPSC line differences in the hepatic differentiation efficiency based on ALB or asialoglycoprotein receptor 1 (ASGR1) expression analysis (Fig. 2*B*). In addition, there were also large inter-PHH-iPS-HLC line differences in ALB or urea secretion capacities (Fig. 2*C*). These results suggest that it is impossible to compare the hepatic characteristics among PHH-iPS-HLCs without compensating for the differences in the hepatic differentiation efficiency. Recently, we developed a method to maintain and proliferate the hepatoblast-like cells (HBCs) generated from human ESCs/iPSCs by using human laminin 111 (LN111) (10). To examine whether the hepatic differentiation efficiency could be made uniform by generating the HLCs following purification and proliferation of the HBCs, the PHH-iPS-HBCs were cultured on LN111 as

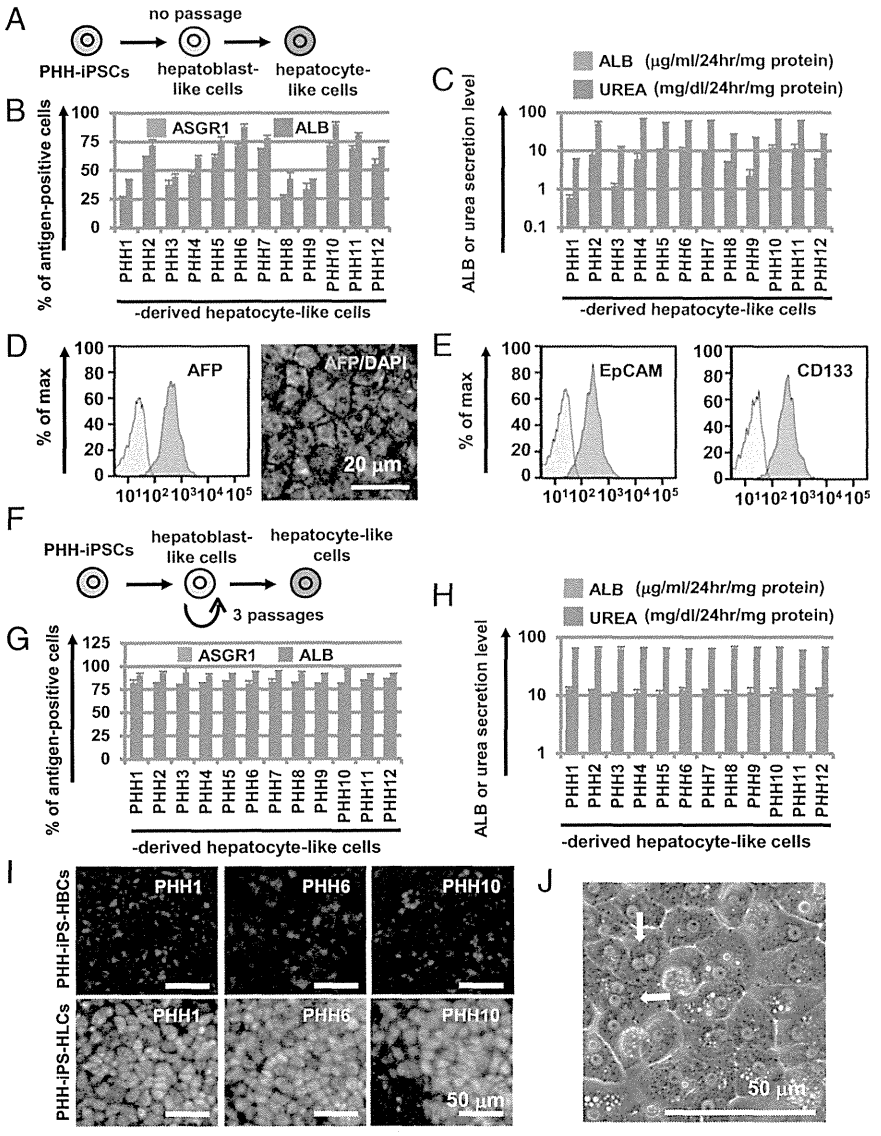

Fig. 2. Highly efficient hepatocyte differentiation from PHH-iPSCs independent of their differentiation tendency. (*A*) PHH-iPSCs were differentiated into the HLCs via the HBCs. (*B*) On day 25 of differentiation, the efficiency of hepatocyte differentiation was measured by estimating the percentage of ASGR1- or ALB-positive cells using FACS analysis. (*C*) The amount of ALB or urea secretion was examined in PHH-iPS-HLCs. (*D*) The percentage of AFP-positive cells in PHH-iPS-HBCs was examined by using FACS analysis (*Left*). The PHH-iPS-HBCs were subjected to immunostaining with anti-AFP (green) antibodies. Nuclei were counterstained with DAPI (blue) (*Right*). (*E*) The percentage of EpCAM- and CD133-positive cells in PHH-iPS-HBCs was examined by using FACS analysis (*Left*). (*F*) PHH-iPSCs were differentiated into the hepatic lineage, and then PHH-iPS-HBCs were purified and maintained for three passages on human LN111. Thereafter, expanded PHH-iPS-HBCs were differentiated into the HLCs. (*G*) The efficiency of hepatic differentiation from PHH-iPS-HBCs was measured by estimating the percentage of ASGR1- or ALB-positive cells using FACS analysis. (*H*) The amount of ALB or urea secretion in PHH-iPS-HLCs was examined. Data represent the mean ± SD from three independent differentiations. (*I*) The PHH1-, 6-, or 10-iPS-HBCs and -HLCs were subjected to immunostaining with anti-αAT (green) antibodies. Nuclei were counterstained with DAPI (blue). (*J*) A phase-contrast micrograph of PHH-iPS-HLCs.

previously described (10), and then differentiated into the HLCs. Almost all of the cells were positive for the hepatoblast marker [alpha-fetoprotein (AFP)] (Fig. 2*D*). In addition, the PHH-iPS-HBCs were positive for two other hepatoblast markers, EpCAM and CD133 (Fig. 2*E*). To examine the hepatic differentiation efficiency of the PHH-iPS-HBCs maintained on LN111-coated dishes for three passages (Fig. 2*F*), the HBCs were differentiated into the HLCs, and then the percentage of ALB- and ASGR1-positive cells was measured by FACS analysis (Fig. 2*G*). All 12 PHH-iPS-HBCs could efficiently differentiate into the HLCs, yielding more than 75% or 85% ASGR1- or ALB-positive cells, respectively. In addition, there was little difference between the PHH-iPSC lines in ALB or urea secretion capacities (Fig. 2*H*). Although there were large differences in the hepatic differentiation capacity among the PHH1/6/10 (Fig. 2*B*), PHH1/6/10-iPS-HBCs could efficiently differentiate into the HLCs that homogeneously expressed αAT (Fig. 2*I*). After the hepatic differentiation of the PHH-iPS-HBCs, the morphology of the HLCs was similar to that of the PHHs: polygonal with distinct round binuclei (Fig. 2*J*). These results indicated that the hepatic differentiation efficiency of the 12 PHH-iPSC lines could be rendered uniform by inducing hepatic maturation after the establishment of self-renewing HBCs. Therefore, we expected that differences in the hepatic characteristics among the HLCs generated from the 12 individual donor PHH-iPS-HBCs could be properly compared. In addition, the hepatic differentiation efficiency could be rendered uniform not only in the PHH-iPSC lines but also in non–PHH-iPSC lines and human ESCs by performing hepatic maturation after the establishment of self-renewing HBCs (*SI Appendix*, Fig. S4). In Figs. 3 and 4, the HLCs were differentiated after the HBC proliferation step to normalize the hepatic differentiation efficiency.

PHH-iPS-HLCs Retained Donor-Specific Drug Metabolism Capacity and Drug Responsiveness. To examine whether the hepatic functions of individual PHH-iPS-HLCs reflect those of individual PHHs, the CYP metabolism capacity and drug responsiveness of PHH-iPS-HLCs were compared with those of PHHs. PHHs are often used as a positive control to assess the hepatic functions of the HLCs, although in all of the previous reports, the donor of PHHs has been different from that of human iPSCs. Because it is generally considered that CYP activity differs widely among individuals, the hepatic functions of the HLCs should be compared with those of genetically identical PHHs to accurately evaluate the hepatic functions of the HLCs. The CYP1A2, -2C9, and -3A4 activity levels in the PHH-iPS-HLCs were ~60% of

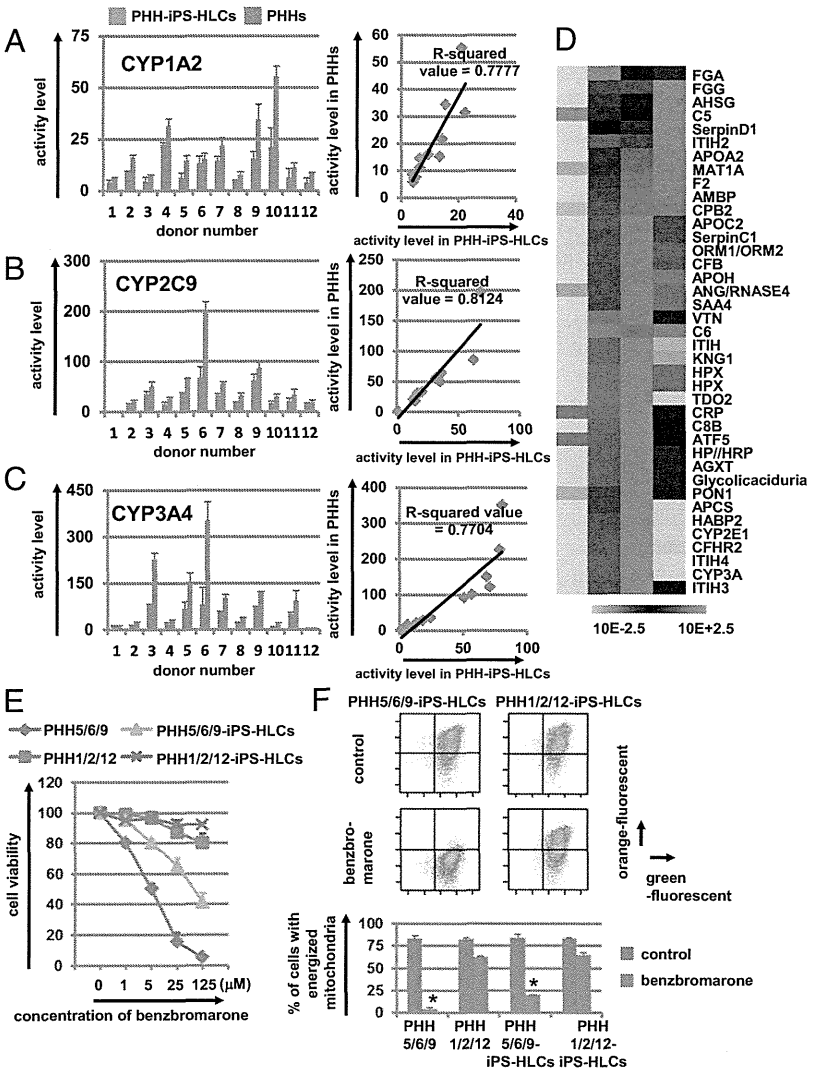

Fig. 3. The drug metabolism capacity and drug responsiveness of PHH-iPS-HLCs were highly correlated with those of their parental PHHs. (*A–C*) CYP1A2 (*A*), -2C9 (*B*), and -3A4 (*C*) activity levels in PHH-iPS-HLCs and PHHs were measured by LC-MS/MS analysis. The R-squared values are indicated in each figure. (*D*) The global gene expression analysis was performed in PHH9-iPSCs, PHH9-iPS-HLCs, PHH9s, and HepG2 (PHH-iPSCs, PHH-iPS-HLCs, and PHHs are genetically identical). Heat-map analyses of liver-specific genes are shown. (*E*) The cell viability of PHH5/6/9, PHH1/2/12, PHH5/6/9-iPS-HLCs, and PHH1/2/12-iPS-HLCs was examined after 24 h exposure to different concentrations of benzbromarone. The cell viability was expressed as a percentage of that in the cells treated only with solvent. (*F*) The percentage of cells with energized mitochondria in the DMSO-treated (control, *Upper*) or benzbromarone-treated (*Lower*) cells based on FACS analysis. Double-positive cells (green+/orange+) represent energized cells, whereas single-positive cells (green+/orange–) represent apoptotic and necrotic cells. Data represent the mean ± SD from three independent experiments (*Lower Graph*). Student *t* test indicated that the percentages in the "control" were significantly higher than those in the "benzbromarone" group ($P < 0.01$). The "PHH5/6/9" represents the average value of cell viability (*E*) or mitochondrial membrane potential (*F*) in PHH5, PHH6, and PHH9. The "PHH1/2/12" represents the average value of cell viability or mitochondrial membrane potential in PHH1, PHH2, and PHH12. PHH5, PHH6, and PHH9 were the top three with respect to CYP2C9 activity levels, whereas PHH1, PHH2, and PHH12 had the lowest CYP2C9 activity levels.

those in the PHHs (Fig. 3 *A–C* and *SI Appendix*, Fig. S5). Interestingly, the CYP1A2, -2C9, and -3A4 activity levels in the PHH-iPS-HLCs were highly correlated with those in the PHHs (the R-squared values were more than 0.77) (Fig. 3 *A*, *B*, and *C*, respectively). These results suggest that it would be possible to predict the individual CYP activity levels through analysis of the CYP activity levels of the PHH-iPS-HLCs. Because the average and variance of CYP3A4 activity levels in PHH-iPS-HLCs, non–PHH-iPS-HLCs, and human ES-HLCs were similar to each other (*SI Appendix*, Fig. S6), the drug metabolism capacity of PHH-iPS-HLCs might be similar to that of nonliver tissue-derived iPS-HLCs and human ES-HLCs. Therefore, it might be possible to predict the diversity of drug metabolism capacity among donors by using nonliver tissue-derived iPS-HLCs and human ES-HLCs as well as PHH-iPS-HLCs. On the other hand, the CYP induction capacities of PHH-iPS-HLCs were weakly correlated with those of PHHs (*SI Appendix*, Fig. S7 *A–C*). To further investigate the characteristics of the HLCs, DNA microarray analyses were performed in genetically identical undifferentiated iPSCs, PHH-iPS-HLCs, and PHHs. The gene expression patterns of liver-specific genes, CYPs, and transporters in the PHH-iPS-HLCs were similar to those in PHHs (Fig. 3*D* and *SI Appendix*, Fig. S7 *D* and *E*, respectively). Next, the hepatotoxic drug responsiveness of PHH-iPS-HLCs was compared with that of PHHs. Benzbromarone, which is known to cause hepatotoxicity by CYP2C9 metabolism (11), was treated to PHH5/6/9 and PHH5/6/9-iPS-HLCs, which have high CYP2C9 activity, or PHH1/2/12 and PHH1/2/12-iPS-HLCs which have low CYP2C9 activity (Fig. 3*E*). The susceptibility of the PHH5/6/9 and PHH5/6/9-iPS-HLCs to benzbromarone was higher than that of PHH1/2/12 and PHH1/2/12-iPS-HLCs, respectively. These results were attributed to the higher CYP2C9 activity levels in PHH5/6/9 and PHH5/6/9-iPS-HLCs compared with those in PHH1/2/12 and PHH1/2/12-iPS-HLCs. Because it is also known that benzbromarone causes mitochondrial toxicity (12), an assay of mitochondrial membrane potential was performed in benzbromarone-treated PHHs and PHH-iPS-HLCs (Fig. 3*F*). The mitochondrial toxicity observed in PHH5/6/9 and PHH5/6/9-iPS-HLCs was more severe than that in PHH1/2/12 and PHH1/2/12-iPS-HLCs, respectively. Taken together, these results suggest that the hepatic functions of the individual PHH-iPS-HLCs were highly correlated with those of individual PHHs.

Interindividual Differences in CYP2D6-Mediated Metabolism and Drug Toxicity, Which Are Caused by SNPs in CYP2D6, Are Reproduced in the PHH-iPS-HLCs. Because certain SNPs are known to have a large impact on CYP activity, the genetic variability of CYP plays an important role in interindividual differences in drug response. CYP2D6 shows the large phenotypic variability due to genetic polymorphism (13). We next examined whether the PHHs used

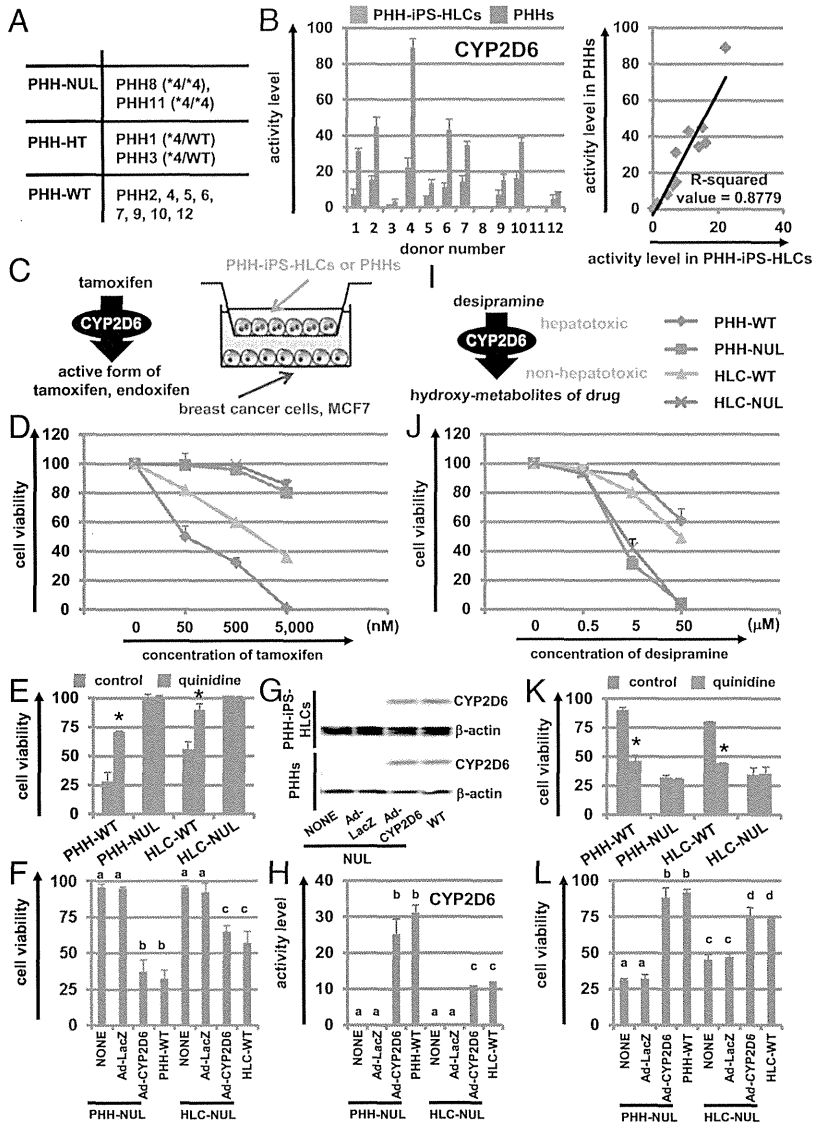

Fig. 4. The interindividual differences in CYP2D6 metabolism capacity and drug responsiveness induced by SNPs in CYP2D6 are reproduced in the PHH-iPS-HLCs. (*A*) SNPs (CYP2D6*3, *4, *5, *6, *7, *8, *16, and *21) in the CYP2D6 gene were analyzed. (*B*) The CYP2D6 activity levels in PHH-iPS-HLCs and PHHs were measured by LC-MS/MS analysis. (*C*) The pharmacological activity of tamoxifen-dependent conversion to its metabolite, endoxifen, by the CYP2D6. The coculture system of breast cancer cells (MCF-7 cells) and the PHH-iPS-HLCs are illustrated. (*D*) The cell viability of MCF-7 cells was assessed after 72-h exposure to different concentrations of tamoxifen. (*E*) The cell viability of MCF-7 cells, which were cocultured with PHH-WT, PHH-NUL, HLC-WT, and HLC-NUL, was assessed after 72-h exposure to 500 nM of tamoxifen in the presence or absence of 3 nM quinidine (a CYP2D6 inhibitor). (*F*) The cell viability of MCF-7 cells cocultured with Ad-CYP2D6-transduced PHH-NUL and HLC-NUL was examined after 72-h exposure to 500 nM of tamoxifen. (*G* and *H*) The CYP2D6 expression (*G*) and activity (*H*) levels in Ad-CYP2D6-transduced PHH-NUL and HLC-NUL were examined by Western blotting and LC-MS/MS analysis. (*I*) The detoxification of desipramine-dependent conversion to its conjugated form by the CYP2D6. (*J*) The cell viability of PHH-WT, PHH-NUL, HLC-WT, and HLC-NUL was assessed after 24-h exposure to different concentrations of desipramine. (*K*) The cell viability of the PHH-WT and HLC-WT was assessed after 24-h exposure to 5 μM of desipramine in the presence or absence of 5 μM of quinidine (a CYP2D6 inhibitor). (*L*) The cell viability of the Ad-CYP2D6-transduced PHH-NUL and HLC-NUL was examined after 24-h exposure to 5 μM of desipramine. The cell viability was expressed as a percentage of that in the cells treated with only solvent. Data represent the mean ± SD from three independent experiments. In *E* and *K*, Student *t* test indicated that the cell viability in the "control" was significantly higher than that in the "quinidine" group ($P < 0.01$). In *F*, *H*, and *L*, statistical significance was evaluated by ANOVA followed by Bonferroni post hoc tests to compare all groups. Groups that do not share the same letter are significantly different from each other ($P < 0.05$).

in this study have the CYP2D6 poor metabolizer genotypes (CYP2D6 *3, *4, *5, *6, *7, *8, *16, and *21) (5). PHH8 and -11 have CYP2D6*4 (null allele), whereas the others have a wild type (WT) or hetero allele (*SI Appendix*, Table S3 and Fig. 4*A*). Consistent with this finding, the PHH8/11-iPS-HLCs also have CYP2D6*4, whereas the others have a wild type or hetero allele. As expected, the CYP2D6 activity levels in the PHH8/11 (PHH-NUL) and PHH8/11-iPS-HLC (HLC-NUL) were significantly lower than those in the PHH-WT and HLC-WT, respectively (Fig. 4*B*). The pharmacological activity of tamoxifen, which is the most widely used agent for patients with breast cancer, is dependent on its conversion to its metabolite, endoxifen, by the CYP2D6 (Fig. 4*C*). To examine whether the pharmacological activity of tamoxifen could be predicted by using PHHs and HLCs that have either the null type CYP2D6*4 allele or wild-type CYP2D6 allele, the breast cancer cell line MCF7 was cocultured with PHHs or HLCs, and then the cells were treated with tamoxifen (Fig. 4*D*). The cell viability of MCF7 cells cocultured with PHHs-NUL or HLCs-NUL was significantly higher than that of MCF7 cells cocultured with PHHs-WT or HLCs-WT. The decrease in cell viability of MCF7 cells cocultured with PHHs-WT or HLCs-WT was rescued by treatment with a CYP2D6 inhibitor, quinidine (Fig. 4*E*). We also confirmed that the cell viability of MCF7 cells cocultured with PHHs-NUL or HLCs-NUL was decreased by CYP2D6 overexpression in the PHHs-NUL or HLCs-NUL (Fig. 4*F*). Note that the expression (Fig. 4*G*) and activity (Fig. 4*H*) levels of CYP2D6 in CYP2D6-expressing adenovirus vector (Ad-CYP2D6)-transduced PHHs-NUL or HLCs-NUL were comparable to those of PHHs-WT or HLCs-WT. These results indicated that the PHHs-WT and HLCs-WT could more efficiently metabolize tamoxifen than the PHHs-NUL and HLCs-NUL, respectively, and thereby induced higher toxicity in MCF7 cells. Similar results were obtained with the other breast cancer cell line, T-47D (*SI Appendix*, Fig. S8 *A–D*). Next, we examined whether the CYP2D6-mediated drug-induced hepatotoxicity could be predicted by using PHHs and HLCs having either a null type CYP2D6*4 allele or wild-type CYP2D6 allele. PHHs and HLCs were treated with desipramine, which is known to cause hepatotoxicity (Fig. 4*I*) (14). The cell viability of PHHs-NUL and HLCs-NUL was significantly lower than that of PHHs-WT and HLCs-WT (Fig. 4*J*). The cell viability of the PHHs-WT or HLCs-WT was decreased by treatment with a CYP2D6 inhibitor, quinidine (Fig. 4*K*). We also confirmed that the decrease in the cell viability of the PHHs-NUL or HLCs-NUL was rescued by CYP2D6 overexpression in the PHHs-NUL or HLCs-NUL (Fig. 4*L*). Similar

results were obtained with the other hepatotoxic drug, perhexiline (*SI Appendix*, Fig. S8 *E–H*). These results indicated that the PHHs-WT and HLCs-WT could more efficiently metabolize imipramine and thereby reduce toxicity compared with the PHHs-NUL and HLCs-NUL. Taken together, our findings showed that the interindividual differences in CYP metabolism capacity and drug responsiveness, which are prescribed by an SNP in genes encoding CYPs, were also reproduced in the PHH-iPS-HLCs.

Discussion

The purpose of this study was to examine whether the individual HLCs could reproduce the hepatic function of individual PHHs. A Yamanaka 4 factor-expressing SeV vector was used in this study to generate integration-free human iPSCs from PHHs. It is known that SeV vectors can express exogenous genes without chromosomal insertion, because these vectors replicate their genomes exclusively in the cytoplasm (15). To examine the different cellular phenotypes associated with SNPs in human iPSC derivatives, the use of integration-free human iPSCs is essential.

We found that the CYP activity levels of the PHH-iPS-HLCs reflected those of parent PHHs, as shown in Fig. 3 *A–C*. There were few interindividual differences in the ratio of CYP expression levels in the PHH-iPS-HLCs to those in PHHs (*SI Appendix*, Fig. S5). Together, these results suggest that it is possible to predict the individual CYP activity levels through analysis of the CYP activity levels of the PHH-iPS-HLCs. In the future, it will be necessary to confirm these results in skin or blood cell-derived iPSCs as well as PHH-iPSCs, although donor-matched PHHs and blood cells (or skin cells) are difficult to obtain. In addition, the comparison of hepatic functions between genetically identical PHHs and PHH-iPS-HLCs (Fig. 3 *A–C*) would enable us to accurately ascertain whether the HLCs exhibit sufficient hepatic function to be a suitable substitute for PHHs in the early phase of pharmaceutical development. Because the drug responsiveness of the individual HLCs reflected that of individual PHHs (Fig. 3 *E* and *F*), it might be possible to perform personalized drug therapy following drug screening using a patient's HLCs. However, the R-squared values of the individual CYP activities differed from each other (Fig. 3 *A–C*), suggesting that the activity levels of some CYPs are largely influenced not only by genetic information but also by environmental factors, such as dietary or smoking habits.

The interindividual differences of CYP2D6 metabolism capacity and drug responsiveness that were prescribed by SNP in genes encoding CYP2D6 were reproduced in the PHH-iPS-HLCs (Fig. 4). It was impossible to perform drug screening in the human hepatocytes derived from a donor with rare SNPs because these hepatocytes could not be obtained. However, because human iPSCs can be generated from such donors with rare SNPs, the CYP metabolism capacity and drug responsiveness of these donors might be possible to predict. Further, it would also be possible to identify the novel SNP responsible for an unexpected hepatotoxicity by using the HLCs in which whole genome sequences are known. We thus believe that the HLCs will be a powerful tool not only for accurate and efficient drug development but also for personalized drug therapy.

Experimental Procedures

DNA Microarray. Total RNA was prepared from the PHH9-iPSCs, PHH9-iPS-HLCs, PHH9, and human hepatocellular carcinoma cell lines by using an RNeasy Mini kit. A pool of three independent samples was used in this study. cRNA amplifying, labeling, hybridizing, and analyzing were performed at Miltenyi Biotec. The Gene Expression Omnibus (GEO) accession no. for the microarray analysis is GSE61287.

Flow Cytometry. Single-cell suspensions of human iPSC-derived cells were fixed with 2% (vol/vol) paraformaldehyde (PFA) for 20 min, and then incubated with the primary antibody (described in *SI Appendix*, Table S1), followed by the secondary antibody (described in *SI Appendix*, Table S2). In case of the intracellular staining, the Permeabilization Buffer (eBioscience) was used to create holes in the membrane thereby allowing the antibodies to enter the cell effectively. Flow cytometry analysis was performed using a FACS LSR Fortessa flow cytometer (BD Biosciences).

ACKNOWLEDGMENTS. We thank Yasuko Hagihara, Natsumi Mimura, and Shigemi Isoyama for their excellent technical support. H.M. and K.K. were supported by grants from the Ministry of Health, Labor, and Welfare. H.M. was also supported by the Project for Technological Development, Research Center Network for Realization of Regenerative Medicine of the Japan Science and Technology Agency and by the Uehara Memorial Foundation. F.S. was supported by the Program for Promotion of Fundamental Studies in Health Sciences of the National Institute of Biomedical Innovation. K.T. and Y.N. were supported by a grant-in-aid for the Japan Society for the Promotion of Science Fellows.

1. Takayama K, et al. (2012) Efficient generation of functional hepatocytes from human embryonic stem cells and induced pluripotent stem cells by HNF4α transduction. *Mol Ther* 20(1):127–137.
2. Medine CN, et al. (2013) Developing high-fidelity hepatotoxicity models from pluripotent stem cells. *Stem Cells Transl Med* 2(7):505–509.
3. Ingelman-Sundberg M (2004) Pharmacogenetics of cytochrome P450 and its applications in drug therapy: The past, present and future. *Trends Pharmacol Sci* 25(4): 193–200.
4. Ingelman-Sundberg M (2001) Genetic susceptibility to adverse effects of drugs and environmental toxicants. The role of the CYP family of enzymes. *Mutat Res* 482(1-2): 11–19.
5. Zhou SF (2009) Polymorphism of human cytochrome P450 2D6 and its clinical significance: Part I. *Clin Pharmacokinet* 48(11):689–723.
6. Borges S, et al. (2006) Quantitative effect of CYP2D6 genotype and inhibitors on tamoxifen metabolism: Implication for optimization of breast cancer treatment. *Clin Pharmacol Ther* 80(1):61–74.
7. Bakke OM, Manocchia M, de Abajo F, Kaitin KI, Lasagna L (1995) Drug safety discontinuations in the United Kingdom, the United States, and Spain from 1974 through 1993: A regulatory perspective. *Clin Pharmacol Ther* 58(1):108–117.
8. Lin T, et al. (2009) A chemical platform for improved induction of human iPSCs. *Nat Methods* 6(11):805–808.
9. Polo JM, et al. (2010) Cell type of origin influences the molecular and functional properties of mouse induced pluripotent stem cells. *Nat Biotechnol* 28(8):848–855.
10. Takayama K, et al. (2013) Long-term self-renewal of human ES/iPS-derived hepatoblast-like cells on human laminin 111-coated dishes. *Stem Cell Reports* 1(4):322–335.
11. McDonald MG, Rettie AE (2007) Sequential metabolism and bioactivation of the hepatotoxin benzbromarone: Formation of glutathione adducts from a catechol intermediate. *Chem Res Toxicol* 20(12):1833–1842.
12. Kaufmann P, et al. (2005) Mechanisms of benzarone and benzbromarone-induced hepatic toxicity. *Hepatology* 41(4):925–935.
13. Ingelman-Sundberg M (2005) Genetic polymorphisms of cytochrome P450 2D6 (CYP2D6): Clinical consequences, evolutionary aspects and functional diversity. *Pharmacogenomics J* 5(1):6–13.
14. Spina E, et al. (1997) Relationship between plasma desipramine levels, CYP2D6 phenotype and clinical response to desipramine: A prospective study. *Eur J Clin Pharmacol* 51(5):395–398.
15. Nishimura K, et al. (2011) Development of defective and persistent Sendai virus vector: A unique gene delivery/expression system ideal for cell reprogramming. *J Biol Chem* 286(6):4760–4771.

OPEN ACCESS Freely available online

PLOS | ONE

HHEX Promotes Hepatic-Lineage Specification through the Negative Regulation of Eomesodermin

Hitoshi Watanabe[1☯], Kazuo Takayama[1,2,3☯], Mitsuru Inamura[1], Masashi Tachibana[1], Natsumi Mimura[2], Kazufumi Katayama[1], Katsuhisa Tashiro[4], Yasuhito Nagamoto[1,2], Fuminori Sakurai[1], Kenji Kawabata[4], Miho Kusuda Furue[5,6], Hiroyuki Mizuguchi[1,2,3,7]*

1 Laboratory of Biochemistry and Molecular Biology, Graduate School of Pharmaceutical Sciences, Osaka University, Osaka, Japan, **2** Laboratory of Hepatocyte Differentiation, National Institute of Biomedical Innovation, Osaka, Japan, **3** iPS Cell-Based Research Project on Hepatic Toxicity and Metabolism, Graduate School of Pharmaceutical Sciences, Osaka University, Osaka, Japan, **4** Laboratory of Stem Cell Regulation, National Institute of Biomedical Innovation, Osaka, Japan, **5** Laboratory of Embryonic Stem Cell Cultures, Department of Disease Bioresources Research, National Institute of Biomedical Innovation, Osaka, Japan, **6** Department of Embryonic Stem Cell Research, Field of Stem Cell Research, Institute for Frontier Medical Sciences, Kyoto University, Kyoto, Japan, **7** The Center for Advanced Medical Engineering and Informatics, Osaka University, Osaka, Japan

Abstract

Human embryonic stem cells (hESCs) could provide a major window into human developmental biology, because the differentiation methods from hESCs mimic human embryogenesis. We previously reported that the overexpression of hematopoietically expressed homeobox (HHEX) in the hESC-derived definitive endoderm (DE) cells markedly promotes hepatic specification. However, it remains unclear how HHEX functions in this process. To reveal the molecular mechanisms of hepatic specification by HHEX, we tried to identify the genes directly targeted by HHEX. We found that HHEX knockdown considerably enhanced the expression level of eomesodermin (EOMES). In addition, HHEX bound to the HHEX response element located in the first intron of EOMES. Loss-of-function assays of EOMES showed that the gene expression levels of hepatoblast markers were significantly upregulated, suggesting that EOMES has a negative role in hepatic specification from the DE cells. Furthermore, EOMES exerts its effects downstream of HHEX in hepatic specification from the DE cells. In conclusion, the present results suggest that HHEX promotes hepatic specification by repressing EOMES expression.

Citation: Watanabe H, Takayama K, Inamura M, Tachibana M, Mimura N, et al. (2014) HHEX Promotes Hepatic-Lineage Specification through the Negative Regulation of Eomesodermin. PLoS ONE 9(3): e90791. doi:10.1371/journal.pone.0090791

Editor: Anton Wutz, Wellcome Trust Centre for Stem Cell Research, United Kingdom

Received May 18, 2013; **Accepted** February 5, 2014; **Published** March 20, 2014

Funding: HM and MKF were supported by grants from the Ministry of Health Labor and Welfare of Japan. HM was also supported by The Uehara Memorial Foundation. FS were supported by Program for Promotion of Fundamental Studies in Health Sciences of the National Institute of Biomedical Innovation (NIBIO). K. Takayama and YN are supported by a Grant-in-aid for the Japan Society for the Promotion of Science Fellows. The funders had no role in study design data collection and analysis decision to publish or preparation of the manuscript.

Competing Interests: The authors have declared that no competing interests exist.

* E-mail: mizuguch@phs.osaka-u.ac.jp

☯ These authors contributed equally to this work.

Introduction

The molecular mechanisms of liver development have been clarified by using model organisms such as chicks, *Xenopus*, *zebrafish*, and mice [1–2]. Although these models have many advantages, the molecular mechanisms of human liver development might be different from those of model organisms. The use of differentiation models from human embryonic stem cells (hESCs) for studying human development might resolve these problems, because these differentiation methods mimic human embryogenesis [3]. Previous reports have demonstrated that the definitive endoderm (DE) cells could be efficiently generated from hESCs in the presence of Activin A [4], and that the hESC-derived DE cells have the potential to differentiate into various DE-derived lineages, such as hepatocytes, pancreatic beta-cells, and small intestinal enterocytes[5–7]. In hepatic differentiation, Agarwal et al. reported that the typical gene expression profiles observed in the differentiation model from hESCs are similar to those observed in fetal liver development [8]. In addition, we previously reported that CCAAT/enhancer binding protein-mediated regulation of TGF beta receptor 2 expression determines the hepatoblast fate decision by using a differentiation model from hESCs [9]. The use of differentiation models from hESCs, rather than the usual model organisms, would provide great opportunities to expand our understanding of the molecular mechanisms.

A transcription factor, *hematopoietically expressed homeobox* (HHEX), is initially expressed in DE, and then its expression is restricted to the future hepatoblasts, which could segregate into both hepatocytes and cholangiocytes [10]. In the *HHEX*-null embryo, some hepatic gene expression levels are reduced and further hepatic development is prevented [11–12]. These studies indicate that the transcription factor HHEX plays an essential role in hepatic specification from DE. Recently, we reported that overexpression of HHEX by using adenovirus (Ad) vectors in the hESC-derived DE cells markedly promotes the hepatic specification [13]. Moreover, Kubo et al. demonstrated that HHEX promotes this process by synergistically working with bone morphogenetic protein 4 (BMP4), and they expected that HHEX might function with *HNF1 homeobox A* (HNF1α) [14], which is known to be its co-activator [15]. However, the functions of HHEX in this process

are not well understood, and the target genes of HHEX have not been investigated in detail. Therefore, we attempted to identify the target genes of HHEX in the hepatic specification by using a differentiation model from hESCs.

In the present study, to elucidate the functions of HHEX in hepatic specification from DE, we attempted to identify the target genes of HHEX by using the hepatic differentiation model from hESCs. To this end, the candidate target gene of HHEX were verified by performing ChIP-qPCR and luciferase reporter assays, and then loss-of-function assays were performed to clarify the functions of the candidate target gene in the hepatic specification. These results confirmed that *eomesodermin* (EOMES), which is known to regulate DE differentiation, is one of the crucial target genes of HHEX in human hepatic specification from the DE. Our report thus shows for the first time that HHEX promotes hepatic specification through the repression of EOMES expression.

Materials and Methods

hESCs Culture

A hESC line, H9 (WA09, WISC Bank, WiCell Research Institute), was maintained on a feeder layer of mitomycin C-treated mouse embryonic fibroblasts (MEF) (Millipore) with ReproStem medium (ReproCELL) supplemented with 5 ng/ml fibroblast growth factor 2 (FGF2) (KATAYAMA CHEMICAL INDUSTRIES). hESCs were dissociated with 0.1 mg/ml dispase (Roche) into small clumps and then were subcultured every 4 or 5 days. H9 was used following the Guidelines for Utilization of Human Embryonic Stem Cells of the Ministry of Education, Culture, Sports, Science and Technology of Japan after approval by the institutional ethical review board at National Institute of Biomedical Innovation.

In vitro Differentiation

The differentiation protocol for the induction of DE cells and hepatoblasts was based on our previous report with some modifications [13–16–21]. Briefly, hESCs were dissociated by using dispase and suspended in MEF-conditioned ReproStem medium supplemented with 10 ng/ml FGF2, and then plated onto a growth factor reduced Matrigel (BD Biosciences)-coated dish. When hESCs reached approximately 80% confluence, the MEF-conditioned ReproStem medium was replaced with the differentiation RPMI-1640 medium (Sigma) containing 100 ng/ml Activin A (R&D systems) (the differentiation RPMI-1640 medium is consisted with RPMI-1640 medium (Sigma) supplemented with B27 supplement (Invitrogen) and 4 mM L-glutamine), and then cultured for 4 days. For induction of the hepatoblasts, the DE cells were cultured for 5 days in the differentiation RPMI-1640 medium supplemented with 20 ng/ml BMP4 (R&D Systems) and 20 ng/ml FGF4 (R&D Systems).

RNA Isolation and Reverse Transcription-PCR

Total RNA was isolated from hESCs and their derivatives using ISOGENE (Nippon Gene). cDNA was synthesized using 500 ng of total RNA with a SuperScript VILO cDNA Synthesis Kit (Invitrogen). Real-time RT-PCR was performed with SYBR Green PCR Master Mix (Applied Biosystems) using an Applied Biosystems StemOnePlus real-time PCR systems. Relative quantification was performed against a standard curve and the values were normalized against the input determined for the housekeeping gene, glyceraldehyde 3-phosphate dehydrogenase (GAPDH). The primer sequences used in this study are described in **Table S1 in File S2**.

Flow Cytometry

Single-cell suspensions of the hESC derivatives were fixed with 2% paraformaldehyde (PFA) at 4°C for 20 minutes and then incubated with the primary antibody, followed by the secondary antibody. Flow cytometry analysis was performed using a FACS LSR Fortessa flow cytometer (BD Biosciences). All the antibodies are listed in **Table S2 in File S2**.

ChIP-qPCR

ChIP assays were performed by using a Chromatin Immunoprecipitation Assay Kit (Millipore) according to the manufacturer's instructions. The hESC-derived cells (approximately 1.0×10^6 cells) were cross-linked with 1% formaldehyde at room temperature for 10 minutes. The cells were washed once with PBS containing protease inhibitors (1 mM phenylmethylsulfonyl fluoride, 1 mg/ml aprotinin and 1 mg/ml pepstatin A) and then harvested using a cell scraper. The cross-linked cells were centrifuged and resuspended with sodium dodecyl sulfate (SDS) lysis buffer with the protease inhibitors described above, and then incubated on ice for 10 minutes. The cells were sonicated to solubilize and shear cross-linked DNA. The resulting whole cells were centrifuged, and the supernatants were diluted in ChIP Dilution Buffer containing the protease inhibitors described above, then added to Protein A magnetic beads and rotated at 4°C for 30 minutes. Next, the supernatants of these cells were immunoprecipitated with anti-human HHEX antibody (Santa Cruz Biotechnology, sc-15129) or anti-goat IgG antibody at 4°C overnight with rotation. On the following day, the resulting supernatants were added to Protein A magnetic beads and rotated at 4°C for 60 minutes, then washed five times with Low Salt Immune Complex Wash Buffer (one time), High Salt Immune Complex Wash Buffer (one time), LiCl Immune Complex Wash Buffer (one time), and TE Buffer (two times) for 5 minutes per wash with rotation. Bound complexes were added to elution buffer (1% SDS, 0.1 M $NaHCO_3$) at room temperature for 15 minutes with rotation, and then the supernatants were added to 5 M NaCl and were eluted at 65°C for 4 hours. Immunoprecipitated DNA was purified by treatment with 0.5 M EDTA, 1 M Tris-HCl, and 10 mg/ml proteinase K at 45°C for 60 minutes and recovered by phenol/chloroform alcohol extraction and ethanol precipitation. Purified DNA was used as a template for qPCR according to the protocol described in the *RNA isolation and reverse transcription-PCR* section above. All the antibodies are listed in **Table S2 in File S2**. The primer sequences used in this study are described in **Table S1 in File S2**.

Plasmid Constructions

The promoter region of EOMES was cloned. To generate the 5′ untranslated region (UTR) of the EOMES-firefly luciferase reporter construct (pGL3-EOM-5UTR1000), a 1,000 bp 5′ UTR of the human EOMES was amplified by using the following primers: 5′-AGCGGTACCTTCCTCTCTACAAACCTTTCCCACTGGG-3′ and 5′-TAACCATGGGCTTTGCAAAGCGCAGACGGCAGCTGGCTGC-3′ (−1,000/−1 5′ UTR of EOMES; KpnI and NcoI restriction sites incorporated into sense and antisense primers, respectively, are underlined) and to generate the long 5′ UTR of the EOMES-firefly luciferase reporter construct (pGL3-EOM-5UTR4000), a 4,000 bp 5′ UTR of the human EOMES was amplified by using the following primers: 5′-CAGGGTACCGATAACACGTTTTTAGTGGGGGTG-3′ and 5′-TAACCATGGGCTTTGCAAAGCGCAGACGGCAGCTGGCTGC-3′ (−4,000/−1−5′ UTR of EOMES; KpnI and NcoI restriction sites incorporated into sense and antisense primers, respectively, are underlined).

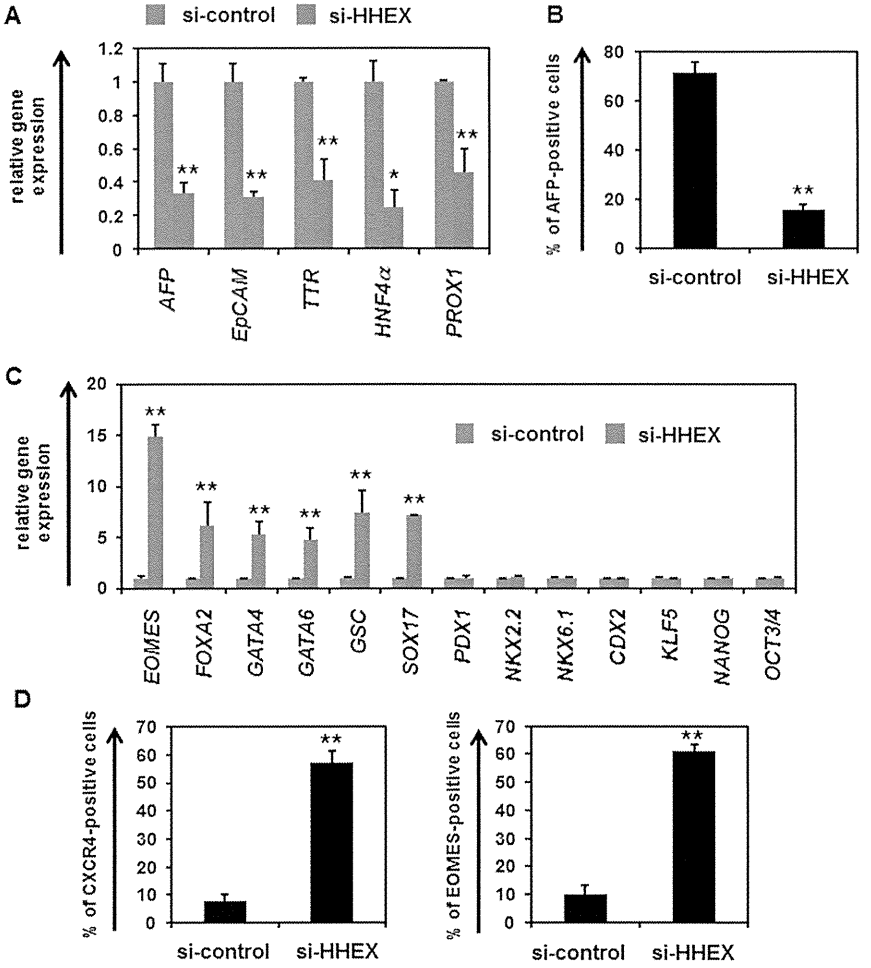

Figure 1. The expression levels of DE markers in the si-HHEX-transfected cells were upregulated in hepatoblast differentiation from DE cells. (**A**) hESCs (H9) were differentiated into DE cells according to the protocol described in the *Materials and Methods* section. The DE cells were transfected with 50 nM si-control or si-HHEX on day 4, and cultured in the medium containing 20 ng/ml BMP4 and 20 ng/ml FGF4 until day 9. On day 9, the gene expression levels of hepatoblast markers (*AFP*, *EpCAM*, *TTR*, *HNF4α*, and *PROX1*) in si-control- or si-HHEX-transfected cells were examined by real-time RT-PCR. The gene expression levels in the si-control-transfected cells were taken as 1.0. (**B**) On day 9, the percentage of AFP-positive cells was measured by using FACS analysis to examine the hepatoblast differentiation efficiency. (**C**) The gene expression levels of DE (*EOMES*, *FOXA2*, *GATA4*, *GATA6*, *GSC*, and *SOX17*), pancreatic (*PDX1*, *NKX2.2*, and *NKX6.1*), intestinal (*CDX2* and *KLF5*), and pluripotent markers (*NANOG* and *OCT3/4*) in the si-control- or si-HHEX-transfected cells were examined by real-time RT-PCR. The gene expression levels in the si-control-transfected cells were taken as 1.0. (**D**) On day 9, the percentage of cells positive for the DE markers (CXCR4 and EOMES) was examined by using FACS analysis. All data are represented as means ± SD ($n = 3$). *$p<0.05$, **$p<0.01$.
doi:10.1371/journal.pone.0090791.g001

Each 5′ UTR of the human EOMES was cloned into the promoter region of the pGL3-Basic vector (Promega) using KpnI and NcoI restriction sites. In addition, the 400 bp region around the HHEX response element (HRE) was amplified by using the following primers: 5′-CCTGCTAGCGTTCTCTGGTACTTTTCAAAATGGTGC-3′ and 5′-GAAAACTAGTATGCGCCTGTGCAAGGGAATAGAATCAG-3′. The 400 bp region around the HRE was cloned into the enhancer region of each of pGL3-EOM-5UTR1000 and pGL3-EOM-5UTR4000 using XbaI restriction site to generate pGL3-EOM-5UTR1000 containing the region around the HRE (p5′ EOM-Luc) and pGL3-EOM-5UTR4000 containing the region around the HRE (pLong-5′ EOM-Luc).

To generate pGL3-EOM-5UTR1000 containing the region which has a mutated HRE reporter construct (p5′ EOM-mut-Luc), the following base substitutions were introduced into the 400 bp region around the HRE: 5′-TCCCAATTAAAATC-3′ to 5′-TCC***AGC***T***G***A***C***AATC-3′. PCR products were cloned into the enhancer region of pGL3-EOM-5UTR1000 using XbaI restriction site.

Luciferase Reporter Assays

HeLa cells were transfected with each of the firefly luciferase reporter plasmids described above (p5′ EOM-Luc or p5′ EOM-mut-Luc) or control plasmids, pGL3-Basic vector plasmids (pControl-Luc), by using Lipofectamine 2000 (Invitrogen)-mediated gene transfection according to the manufacturer's instructions. HeLa cells were seeded at a density of 2.0×10^5 cells/well in 24-well tissue culture plates, and cultured for 24 hours before transfection. HeLa cells were transfected with 333 ng/well of each firefly luciferase reporter plasmids (pControl-Luc, p5′ EOM-Luc, or p5′ EOM-mut-Luc), 333 ng/well of HHEX expression plasmids (pHMEF5-HHEX [13]) or blank expression plasmids (pHMEF5), and 333 ng/well of internal control plasmids (pCMV-

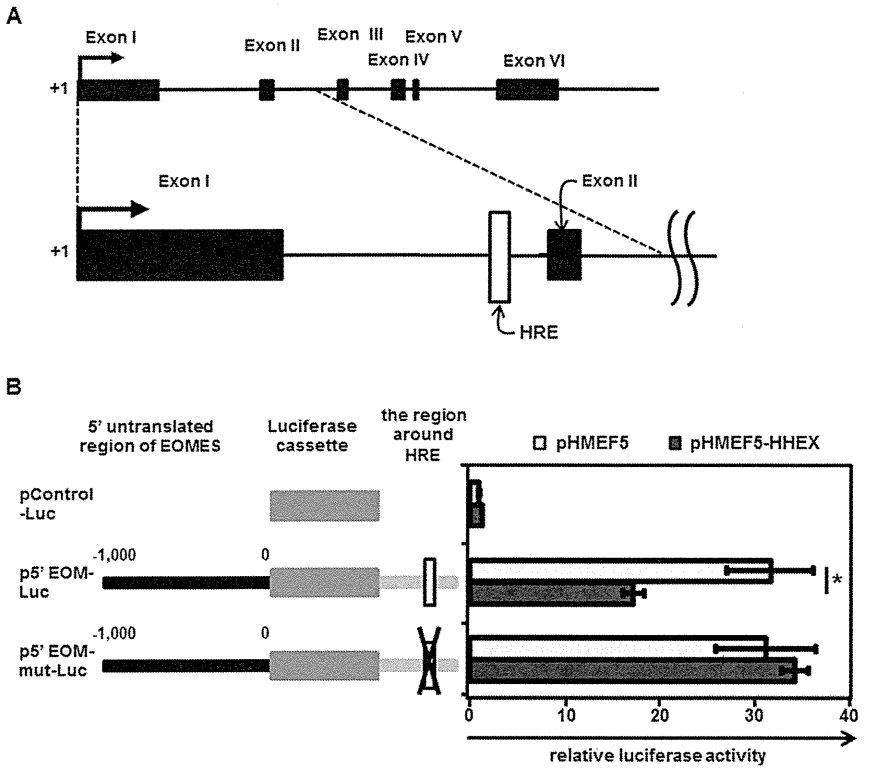

Figure 2. HHEX suppresses EOMES expression by binding to the HRE located in the first intron of EOMES. (**A**) An overview of the EOMES mRNA precursor and the location of the putative HRE are presented. The HRE is located in the first intron of EOMES. (**B**) Luciferase reporter assays were performed to examine the regulation of EOMES expression by HHEX. HeLa cells were cotransfected with both firefly luciferase reporter plasmids (pControl-Luc, p5′ EOM-Luc, or p5′ EOM-mut-Luc) and effecter plasmids (control plasmids (pHMEF5) or HHEX expression plasmids (pHMEF5-HHEX)). The details of the luciferase reporter assays are described in the *Materials and Methods* section. The luciferase activities in the pControl-Luc- and pHMEF5-cotransfected cells were taken as 1.0. All data are represented as means ± SD ($n = 3$). *, $p<0.05$.
doi:10.1371/journal.pone.0090791.g002

Renilla luciferase), and cultured for 72 hours. The luciferase activities in the cells were measured by using Dual Luciferase Assay System (Promega) according to the manufacturer's instructions. Firefly luciferase activities in the cells were normalized by the measurement of renilla luciferase activities. The luciferase activity in the cells cotrasfected with pControl-Luc and pHMEF5 was assigned a value of 1.0.

siRNA Transfection

Knockdown of HHEX or EOMES was performed using a specific small interfering RNA (siRNA) fourplex set targeted to HHEX or EOMES, respectively (Darmacon SMARTpool) (Thermo Fisher Scientific). Si-Control (Darmacon siGENOME Non-Targeting siRNA Pool) (Thermo Fisher Scientific) was used as a control. Lipofectamine RNAiMAX (Invitrogen)-mediated gene transfection was used for the reverse transfection according to the manufacturer's instructions. The hESC-derived DE cells on day 4 were transfected with 50 nM of siRNA for 6 hours by reverse transfection.

Immunohistochemistry

The hESC-derived cells were fixed with methanol or 4% PFA. After blocking with PBS containing 1% BSA (Sigma), 0.2% Triton X-100 (Sigma), and 10% FBS, the cells were incubated with primary antibody at 4°C overnight, followed by incubation with a secondary antibody that was labeled with Alexa Fluor 488 (Invitrogen) at room temperature for 1 hour. All the antibodies are listed in **Table S2 in File S2**.

Western Blotting Analysis

The hESC-derived cells were homogenized with lysis buffer (20 mM HEPES, 2 mM EDTA, 10% glycerol, 0.1% SDS, 1% sodium deoxycholate, and 1% Triton X-100) containing a protease inhibitor mixture (Sigma). After being frozen and thawed, the homogenates were centrifuged at 15,000 *g* at 4°C for 10 minutes, and the supernatants were collected. The lysates were subjected to SDS-PAGE on 7.5% polyacrylamide gel and were then transferred onto polyvinylidene fluoride membranes (Millipore). After the reaction was blocked with 1% skim milk in TBS containing 0.1% Tween 20 at room temperature for 1 hour, the membranes were incubated with anti-human HHEX, EOMES, or β-actin antibodies at 4°C overnight, followed by reaction with horseradish peroxidaseconjugated anti-rabbit IgG or anti-mouse IgG antibodies at room temperature for 1 hour. The band was visualized by ECL Plus Western blotting detection reagents (GE Healthcare) and the signals were read using an LAS-4000 imaging system (Fuji Film). All the antibodies are listed in **Table S2 in File S2**.

Results

Obstruction of Hepatoblast Differentiation by HHEX Knockdown Results in Upregulation of the Expression Levels of DE Markers

It is known that HHEX plays an important role in hepatoblast differentiation [11–12–14]. We have previously reported that HHEX overexpression promoted hepatoblast differentiation from

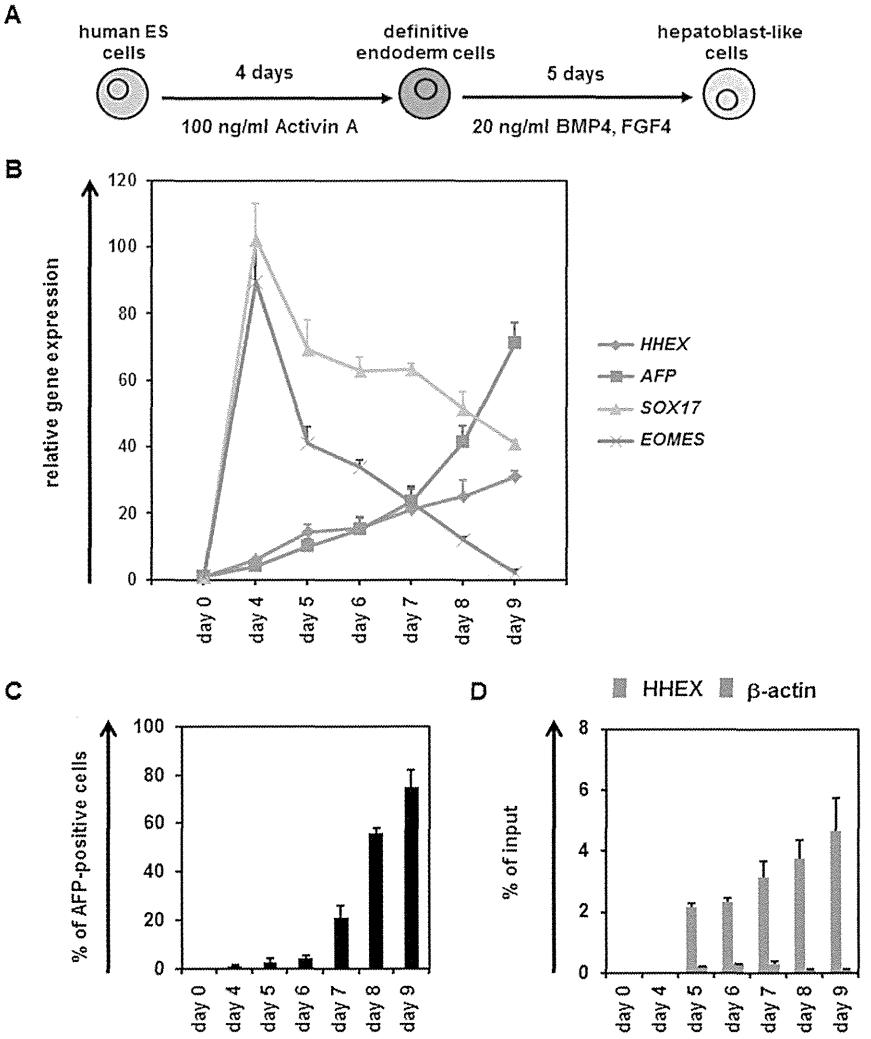

Figure 3. Temporal analysis of endogenous gene expression levels of EOMES and HHEX in hepatoblast differentiation from hESCs. (**A**) The schematic protocol for hepatoblast differentiation from hESCs (H9) is shown. (**B**) The temporal gene expression levels of *HHEX, AFP, SOX17* and *EOMES* were examined by real-time RT-PCR in hepatoblast differentiation. The gene expression levels in undifferentiated hESCs were taken as 1.0. (**C**) To examine the hepatoblast differentiation efficiency, the percentage of AFP-positive cells was measured by FACS analysis. (**D**) The HHEX protein-binding frequencies of the regions around the HRE of the EOMES gene and a negative control gene (β-ACTIN) were measured by ChIP-qPCR analysis. The results are presented as the percent input of anti-HHEX samples compared with those of anti-IgG samples. All data are represented as means ± SD ($n = 3$).

doi:10.1371/journal.pone.0090791.g003

the hESC-derived DE cells [13]. To confirm the importance of HHEX in hepatoblast differentiation, a loss of function assay of HHEX was performed by using siRNA-mediated HHEX knockdown. We confirmed the knockdown of HHEX expression in the hESC-derived DE cells that has been transfected with si-HHEX (**Fig. S1 in File S1**). The gene expression levels of hepatoblast markers in the si-HHEX-transfected cells were significantly downregulated as compared with those in the si-control-transfected cells (**Fig. 1A**). In addition, the percentage of alpha-fetoprotein (AFP; a hepatoblast marker)-positive cells was decreased by HHEX knockdown on day 9 (**Fig. 1B**). These results suggest that hepatoblast differentiation is prevented by HHEX knockdown, demonstrating that HHEX plays an important role in hepatoblast differentiation from DE cells. To characterize the si-HHEX-transfected cells on day 9, the gene expression levels of DE, pancreatic, intestinal, and pluripotent markers were examined (**Fig. 1C**). Interestingly, the gene expression levels of DE markers were significantly upregulated by HHEX knockdown, although those of pancreatic, intestinal, and pluripotent markers were not changed by HHEX knockdown. Furthermore, the percentage of DE marker (CXCR4 and EOMES)-positive cells was increased by HHEX knockdown (**Fig. 1D**). In addition, the percentage of AFP-positive cells or *EOMES* expression level was decreased or increased, respectively, by HHEX knockdown not only in the DE cells (day 4) but also in the cells starting to commit to hepatoblast (day 5–7) (**Fig. S2 in File S1**). This suggested that HHEX knockdown inhibits hepatoblast differentiation but does not simply change the number of the DE cells. These results suggest that the inhibition of HHEX expression during hepatoblast differentiation results in an increase of DE cells, but not pancreatic, intestinal, or undifferentiated cells.

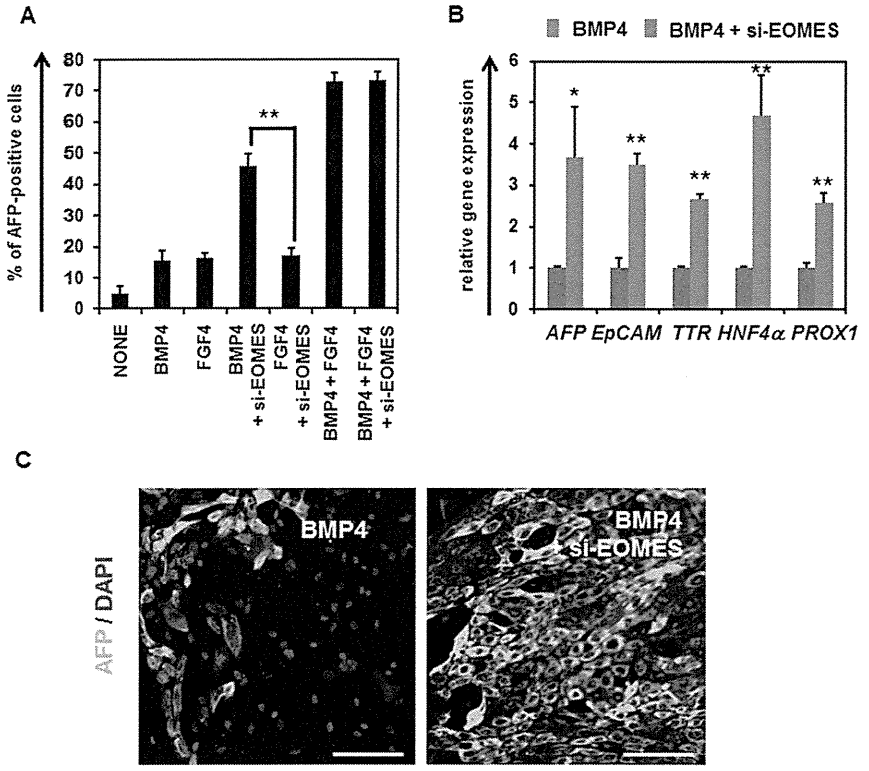

Figure 4. Hepatoblast differentiation was promoted by knockdown of EOMES in the presence of BMP4. (**A**) The hESCs (H9) were differentiated into the DE cells according to the protocol described in the *Materials and Methods* section. The hESC-derived DE cells were transfected with 50 nM si-control or si-EOMES on day 4, and then cultured with the medium containing BMP4 or FGF4. The percentage of AFP-positive cells was examined by FACS analysis on day 9. (**B**) The gene expression levels of hepatoblast markers (*AFP*, *EpCAM*, *TTR*, *HNF4α*, and *PROX1*) were measured by real-time RT-PCR on day 9. The gene expression levels in si-control-transfected cells were taken as 1.0. (**C**) The si-control- or si-EOMES-transfected cells were subjected to immunostaining with anti-AFP (green) antibodies. Nuclei were counterstained with DAPI (blue). The bar represents 50 μm. All data are represented as means ± SD ($n=3$). *$p<0.05$, **$p<0.01$.
doi:10.1371/journal.pone.0090791.g004

HHEX Directly Represses EOMES Expression

Because the gene expression level of *EOMES* was most increased by HHEX knockdown in hepatoblast differentiation, we expected that EOMES might be directly regulated by HHEX. The putative HHEX-binding site (HHEX response element (HRE)) [22] was found in the first intron of EOMES as shown in **Figure 2A**. To investigate whether HHEX could directly repress EOMES transcription, luciferase reporter assays were performed. The reporter plasmids that contain a 5′ untranslated region (UTR) of EOMES (**Fig. S3 in File S1**) and the first intron of EOMES were generated because the putative HHEX-binding site was observed in the first intron of EOMES. The luciferase reporter assays showed that p5' EOM-Luc, which contains the wild-type HRE, mediates significant repression of luciferase activity by HHEX overexpression, whereas p5' EOM-mut-Luc, which contains a mutant HRE, mediates similar luciferase activity even in the presence of HHEX (**Fig. 2B**). These results indicated that HHEX represses EOMES expression through the HRE located in the first intron of EOMES.

Endogenous Temporal Gene Expression Analysis of HHEX and EOMES in Hepatic Specification

To examine the relationship between HHEX and EOMES in hepatic specification, the temporal gene expression patterns of *HHEX* and *EOMES* were examined in hepatoblast differentiation from hESCs (**Fig. 3A**). In DE differentiation (from day 0 to 4), the gene expression levels of *EOMES* and *SOX17* were increased, although those of *HHEX* and *AFP* did not change (**Fig. 3B**). In the hepatic specification process (from day 5 to 9), the gene expression levels of *HHEX* and *AFP* began to be upregulated on day 5, and continued to increase until day 9. On the other hand, the gene expression levels of *EOMES* and *SOX17* started to decrease on day 5, and continued to decrease until day 9. We confirmed that the percentage of CXCR4-positive cells was 95.2±2.2% on day4. In addition, we confirmed that few AFP-positive cells were observed on day 5, and that the percentage of AFP-positive cells continuously increased until day 9 (**Fig. 3C**). To examine whether HHEX binds to the HRE located in the first intron of EOMES, ChIP-qPCR analysis of hepatoblast differentiation from hESCs was performed (**Fig. 3D**). HHEX bound to the HRE located in the first intron of EOMES on day 5, when the hepatic specification began. The amount of HHEX binding to that site continued to increase until day 9. These results suggest that HHEX binds to HRE located in the first intron of EOMES in hepatic specification from the DE cells.

EOMES Knockdown Promotes Hepatic Specification in the Presence of BMP4

To examine the function of EOMES in hepatoblast differentiation, EOMES was knocked down in the DE cells in the presence of BMP4 or FGF4. We confirmed the knockdown of EOMES expression in the hESC-derived DE cells that has been transfected with si-EOMES (**Fig. S4 in File S1**). Although the percentage of AFP-positive cells was increased by EOMES knockdown in the

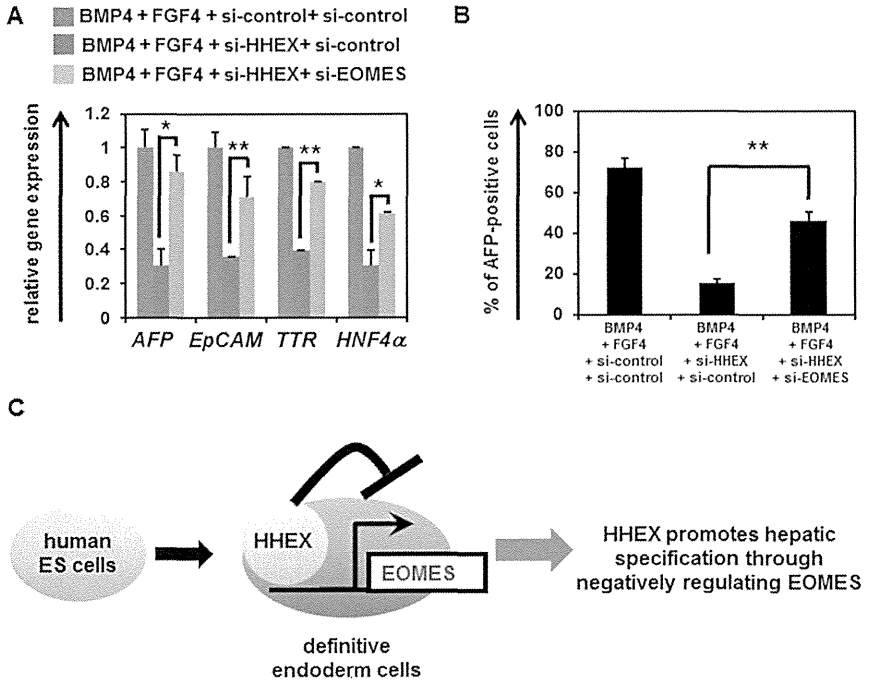

Figure 5. Hepatoblast differentiation is inhibited by EOMES, which functions downstream of HHEX. (**A**) The hESCs (H9) were differentiated into the DE cells according to the protocol described in the *Materials and Methods* section. The hESC-derived DE cells were transfected with 50 nM si-control, si-EOMES, or si-HHEX on day 4, and then cultured with the medium containing BMP4 and FGF4. The gene expression levels of hepatoblast markers (*AFP*, *EpCAM*, *TTR*, and *HNF4α*) were measured by real-time RT-PCR on day 9. The gene expression levels in si-control- and si-HHEX-transfected cells were taken as 1.0. (**B**) The percentage of AFP-positive cells was examined by FACS analysis on day 9. All data are represented as means ± SD ($n=3$). *$p<0.05$, **$p<0.01$. (**C**) HHEX promotes the hepatic specification from the hESC-derived DE cells by negatively regulating EOMES expression. A model of the hepatic specification from the hESC-derived DE cells by HHEX is presented. In the hESC-derived DE cells, HHEX represses EOMES expression. In this way, HHEX promotes the hepatic specification from the hESC-derived DE cells.
doi:10.1371/journal.pone.0090791.g005

presence of BMP4, it was not changed by EOMES knockdown in the presence of FGF4 (**Fig. 4A**). In addition, EOMES knockdown did not affect the percentage of AFP-positive cells in the presence of both FGF4 and BMP4. This might have been because the endogenous *EOMES* expression level was already sufficiently suppressed under the existence of FGF4 (**Fig. S5 in File S1**). To further investigate the function of EOMES in hepatoblast differentiation, gene expression and immunohistochemical analyses of hepatoblast markers were performed in si-EOMES-transfected cells. The gene expression levels of hepatoblast markers in si-EOMES-transfected cells were upregulated as compared with those in si-control-transfected cells (**Fig. 4B**). Consistently, the immunohistochemical analysis of AFP showed that EOMES knockdown upregulated the expression levels of AFP (**Fig. 4C**). In addition, EOMES knockdown increased the percentage of AFP-positive cells not only in the DE cells (day 4) but also in the cells starting to commit to hepatoblast (day 5–7) (**Fig. S6 in File S1**). This suggested that EOMES knockdown promotes hepatoblast differentiation but does not simply change the number of the DE cells. These results suggest that hepatic specification from the DE cells is promoted by EOMES knockdown depending on the existence of BMP4.

EOMES Functions Downstream of HHEX in the Hepatic Specification from the DE Cells

To examine whether EOMES functions downstream of HHEX in the hepatic specification from the DE cells, both HHEX and EOMES were knocked down in the DE cells, and then the gene expression profiles of hepatoblast markers were analyzed. The gene expression levels of hepatoblast markers were upregulated in both si-HHEX- and si-EOMES-transfected cells as compared with those in si-HHEX-transfected cells (**Fig. 5A**). Furthermore, the percentage of AFP-positive cells was also increased by double-knockdown of HHEX and EOMES (**Fig. 5B**). These results suggest that EOMES knockdown could promote the hepatic specification from the DE cells by HHEX knockdown. In conclusion, EOMES exerts downstream of HHEX in the hepatic specification from the DE cells.

Discussion

The purpose of this study was to identify and characterize the target genes of HHEX in hepatic specification from DE to elucidate the functions of HHEX in this process. We clearly demonstrated that the expression of EOMES is directly suppressed by HHEX, and that EOMES is one of the crucial target genes of HHEX in the hepatic specification from the hESC-derived DE cells. We also showed that EOMES knockdown in the hESC-derived DE cells could rescue the si-HHEX-mediated inhibition of hepatic specification. Our findings indicate that promotion of the hepatic specification by HHEX in the hESC-derived DE cells would be mainly mediated by the repression of EOMES expression (**Fig. 5C**).

To explore direct target genes of HHEX in the hepatic specification, EOMES knockdown experiments were conducted (**Fig. 1**). The luciferase reporter assays (**Fig. 2B**) and ChIP-qPCR (**Fig. 3C**) indicated that HHEX represses EOMES expression by binding to the first intron of EOMES containing a putative HRE. It might be expected that HHEX recruits co-repressor proteins to

repress EOMES expression because HHEX could negatively regulate the expressions of target genes such as *vascular endothelial growth factor (Vegf)* and *vascular endothelial growth factor receptor-1 (Vegfr-1)* by forming the co-repressor protein complexes [23–25]. Previous studies demonstrated that HHEX has three main domains, a repression domain, a DNA-binding domain, and an activation domain [26], and thus exerts both positive and negative effects on the target gene expressions. Taken together, these findings suggested that HHEX would repress EOMES expression through the function of its repression domain.

The results in **figure 4A** demonstrate that EOMES knockdown promoted hepatic specification in the presence of BMP4, but not FGF4. Because it was previously reported that FGF4 could induce the expression level of HHEX in the DE cells [27], FGF4 treatment in the DE cells would lead to downregulation of EOMES expression via the regulation of HHEX expression. Therefore, HHEX and EOMES might exert in the downstream of FGF4 in the hepatic specification. In addition, both BMP4 and FGF4 are necessary for hepatic specification (**Fig. 4A**). However, the functions of BMP4 in hepatic specification and the synergistic effect of BMP and FGF have not been sufficiently elucidated, and will need to be resolved in future studies.

Simultaneous knockdown of HHEX and EOMES in the hESC-derived DE cells led to rescue of the HHEX-mediated inhibition of the hepatic specification (**Fig. 5**). These results suggested that the majority of functions in the hepatic specification by HHEX may be caused by the repression of EOMES expression. EOMES is known to regulate numerous target genes related to DE differentiation, and thus the repression of EOMES expression might also promote other DE-derived lineage specifications, such as pancreatic specification. HHEX is known to regulate not only hepatic specification but also pancreatic specification [11–28]. Therefore, EOMES might also be a target gene of HHEX in pancreatic specification as well as in hepatic specification. Because the HHEX protein is known to interact with the HNF1α protein and synergistically upregulate the HNF1α target gene expression [15], it would be of interest to examine the relationship between HHEX and HNF1α in the hepatic specification from the hESC-derived DE cells. The proteomic analyses of HHEX protein in the hepatic specification from the hESC-derived DE cells might help to elucidate the functions of HHEX in this process.

Conclusions

In summary, we showed that the homeobox gene HHEX promotes the hepatic-lineage specification from the hESC-derived DE cells through the repression of EOMES expression. Previously, we reported that transduction of SOX17, HNF4α, FOXA2 or HNF1α into the hESC-derived cells could promote efficient hepatic differentiation [16–18]. The direct target genes of these genes might be identified by using the strategy described here. Furthermore, identification of the genes targeted by functional genes in the various lineage differentiation models from hESCs will promote understanding of the intricate transcriptional networks that regulate human development.

Supporting Information

File S1 Contains the following files: **Figure S1. Knockdown of HHEX in the DE cells by si-HHEX transfection. (A, B)** The hESCs (H9) were differentiated into the DE cells (day 4) according to the protocol described in *Materials and Methods* section. The DE cells were transfected with 50 nM si-control or si-HHEX on day 4. On day 6, the HHEX expression levels in si-control- or si-HHEX-transfected cells were examined by real-time RT-PCR (**A**) or Western blotting (**B**). The gene expression levels of *HHEX* in the si-control-transfected cells were taken as 1.0. All data are represented as means ± SD ($n = 3$). ** $p<0.01$. **Figure S2. The percentage of AFP-positive cells or *EOMES* expression level was decreased or increased, respectively, by HHEX knockdown. (A, B)** The hESCs (H9) were differentiated into the DE cells according to the protocol described in the *Materials and Methods* section. The DE cells were transfected with 50 nM si-control or si-HHEX on day 4, 5, 6, or 7, and cultured in medium containing 20 ng/ml BMP4 and 20 ng/ml FGF4 until day 9. On day 9, the percentage of AFP-positive cells was measured by using FACS analysis to examine the hepatoblast differentiation efficiency (**A**). Also on day 9, the gene expression levels of EOMES in si-control- or si-HHEX-transfected cells were examined by real-time RT-PCR (**B**). The gene expression levels in the si-control-transfected cells were taken as 1.0. All data are represented as means ± SD ($n = 3$). **$p<0.01$. **Figure S3. Both 1,000 bp and 4,000 bp 5′ UTR of EOMES have promoter activities.** Luciferase reporter assays were performed to examine whether 1,000 bp and 4,000 bp 5′ UTR of EOMES have promoter activity. HeLa cells were cotransfected with both 500 ng/well of firefly luciferase reporter plasmids (pControl-Luc, p5' EOM-Luc, or pLong-5′ EOM-Luc), and 500 ng/well of internal control plasmids (pCMV-Renilla luciferase), and cultured for 72 hours. The luciferase activities in the cells were measured by using Dual Luciferase Assay System (Promega) according to the manufacturer's instructions. Firefly luciferase activities in the cells were normalized by the measurement of renilla luciferase activities. The RLU in the pControl-Luc-transfected cells was assigned a value of 1.0. All data are represented as means ± SD ($n = 3$). *, $p<0.05$. **Figure S4. Knockdown of EOMES in the DE cells by si-EOMES transfection. (A, B)** The hESCs (H9) were differentiated into the DE cells (day 4) according to the protocol described in *Materials and Methods* section. The DE cells were transfected with 50 nM si-control or si-EOMES on day 4. On day 6, the EOMES expression levels in si-control- or si-EOMES-transfected cells were examined by real-time RT-PCR (**A**) or Western blotting (**B**). The gene expression levels of *EOMES* in the si-control-transfected cells were taken as 1.0. All data are represented as means ± SD ($n = 3$). ** $p<0.01$. **Figure S5. Hepatoblast differentiation was promoted by knockdown of EOMES.** The hESCs (H9) were differentiated into the DE cells according to the protocol described in the *Materials and Methods* section. The hESC-derived DE cells were transfected with 50 nM si-control or si-EOMES on day 4, 5, 6, or 7, and then cultured in medium containing BMP4 or FGF4. The percentage of AFP-positive cells was examined by FACS analysis on day 9. All data are represented as means ± SD ($n = 3$). **$p<0.01$. **Figure S6. The *EOMES* or *HHEX* expression level was suppressed or increased, respectively, in the presence of FGF4.** The hESCs (H9) were differentiated into the DE cells according to the protocol described in the *Materials and Methods* section. The hESC-derived DE cells were cultured in medium containing BMP4 or FGF4 until day 9. The gene expression levels of *EOMES*, *HHEX*, or *AFP* in the non-treated cells (control) were taken as 1.0. All data are represented as means ± SD ($n = 3$). **$p<$ 0.01 (compared with control).
(PDF)

File S2 Contains the following files: **Table S1.** List of primers used in this study. **Table S2.** List of antibodies used in this study.
(DOC)

Acknowledgments

We thank Yasuko Hagihara, Misae Nishijima, Nobue Hirata, and Reiko Hirabayashi for their excellent technical support.

Author Contributions

Conceived and designed the experiments: HW K. Takayama MI MT K. Katayama K. Kawabata HM. Performed the experiments: HW K. Takayama MI NM. Analyzed the data: HW K. Takayama MI MT K. Katayama K. Tashiro YN FS K. Kawabata MKF HM. Wrote the paper: HW K. Takayama HM. Contributed equally to this work: HW K. Takayama.

References

1. Zaret KS, Grompe M (2008) Generation and regeneration of cells of the liver and pancreas. Science 322: 1490–1494.
2. Si-Tayeb K, Lemaigre FP, Duncan SA (2010) Organogenesis and development of the liver. Dev Cell 18: 175–189.
3. Thomson JA, Itskovitz-Eldor J, Shapiro SS, Waknitz MA, Swiergiel JJ, et al. (1998) Embryonic stem cell lines derived from human blastocysts. Science 282: 1145–1147.
4. D'Amour KA, Agulnick AD, Eliazer S, Kelly OG, Kroon E, et al. (2005) Efficient differentiation of human embryonic stem cells to definitive endoderm. Nat Biotechnol 23: 1534–1541.
5. D'Amour KA, Bang AG, Eliazer S, Kelly OG, Agulnick AD, et al. (2006) Production of pancreatic hormone-expressing endocrine cells from human embryonic stem cells. Nat Biotechnol 24: 1392–1401.
6. Si-Tayeb K, Noto FK, Nagaoka M, Li J, Battle MA, et al. (2010) Highly efficient generation of human hepatocyte-like cells from induced pluripotent stem cells. Hepatology 51: 297–305.
7. Spence JR, Mayhew CN, Rankin SA, Kuhar MF, Vallance JE, et al. (2011) Directed differentiation of human pluripotent stem cells into intestinal tissue in vitro. Nature 470: 105–109.
8. Agarwal S, Holton KL, Lanza R (2008) Efficient differentiation of functional hepatocytes from human embryonic stem cells. Stem Cells 26: 1117–1127.
9. Takayama K, Kawabata K, Nagamoto Y, Inamura M, Ohashi K, et al. (2014) CCAAT/enhancer binding protein-mediated regulation of TGFbeta receptor 2 expression determines the hepatoblast fate decision. Development 141: 91–100.
10. Bogue CW, Ganea GR, Sturm E, Ianucci R, Jacobs HC (2000) Hex expression suggests a role in the development and function of organs derived from foregut endoderm. Dev Dyn 219: 84–89.
11. Bort R, Signore M, Tremblay K, Martinez Barbera JP, Zaret KS (2006) Hex homeobox gene controls the transition of the endoderm to a pseudostratified, cell emergent epithelium for liver bud development. Dev Biol 290: 44–56.
12. Keng VW, Yagi H, Ikawa M, Nagano T, Myint Z, et al. (2000) Homeobox gene Hex is essential for onset of mouse embryonic liver development and differentiation of the monocyte lineage. Biochem Biophys Res Commun 276: 1155–1161.
13. Inamura M, Kawabata K, Takayama K, Tashiro K, Sakurai F, et al. (2011) Efficient Generation of Hepatoblasts From Human ES Cells and iPS Cells by Transient Overexpression of Homeobox Gene HEX. Mol Ther 19: 400–407.
14. Kubo A, Kim YH, Irion S, Kasuda S, Takeuchi M, et al. (2010) The homeobox gene Hex regulates hepatocyte differentiation from embryonic stem cell-derived endoderm. Hepatology 51: 633–641.
15. Tanaka H, Yamamoto T, Ban T, Satoh S, Tanaka T, et al. (2005) Hex stimulates the hepatocyte nuclear factor 1alpha-mediated activation of transcription. Arch Biochem Biophys 442: 117–124.
16. Takayama K, Inamura M, Kawabata K, Tashiro K, Katayama K, et al. (2011) Efficient and Directive Generation of Two Distinct Endoderm Lineages from Human ESCs and iPSCs by Differentiation Stage-Specific SOX17 Transduction. PLoS One 6: e21780.
17. Takayama K, Inamura M, Kawabata K, Katayama K, Higuchi M, et al. (2012) Efficient Generation of Functional Hepatocytes From Human Embryonic Stem Cells and Induced Pluripotent Stem Cells by HNF4alpha Transduction. Mol Ther 20: 127–137.
18. Takayama K, Inamura M, Kawabata K, Sugawara M, Kikuchi K, et al. (2012) Generation of metabolically functioning hepatocytes from human pluripotent stem cells by FOXA2 and HNF1alpha transduction. J Hepatol 57: 628–636.
19. Takayama K, Kawabata K, Nagamoto Y, Kishimoto K, Tashiro K, et al. (2013) 3D spheroid culture of hESC/hiPSC-derived hepatocyte-like cells for drug toxicity testing. Biomaterials 34: 1781–1789.
20. Nagamoto Y, Tashiro K, Takayama K, Ohashi K, Kawabata K, et al. (2012) The promotion of hepatic maturation of human pluripotent stem cells in 3D co-culture using type I collagen and Swiss 3T3 cell sheets. Biomaterials 33: 4526–4534.
21. Takayama K, Nagamoto Y, Mimura N, Tashiro K, Sakurai F, et al. (2013) Long-Term Self-Renewal of Human ES/iPS-Derived Hepatoblast-like Cells on Human Laminin 111-Coated Dishes. Stem Cell Reports 1: 322–335.
22. Cong R, Jiang X, Wilson CM, Hunter MP, Vasavada H, et al. (2006) Hhex is a direct repressor of endothelial cell-specific molecule 1 (ESM-1). Biochem Biophys Res Commun 346: 535–545.
23. Noy P, Williams H, Sawasdichai A, Gaston K, Jayaraman PS (2010) PRH/Hhex controls cell survival through coordinate transcriptional regulation of vascular endothelial growth factor signaling. Mol Cell Biol 30: 2120–2134.
24. Guiral M, Bess K, Goodwin G, Jayaraman PS (2001) PRH represses transcription in hematopoietic cells by at least two independent mechanisms. J Biol Chem 276: 2961–2970.
25. Swingler TE, Bess KL, Yao J, Stifani S, Jayaraman PS (2004) The proline-rich homeodomain protein recruits members of the Groucho/Transducin-like enhancer of split protein family to co-repress transcription in hematopoietic cells. J Biol Chem 279: 34938–34947.
26. Crompton MR, Bartlett TJ, MacGregor AD, Manfioletti G, Buratti E, et al. (1992) Identification of a novel vertebrate homeobox gene expressed in haematopoietic cells. Nucleic Acids Res 20: 5661–5667.
27. Morrison GM, Oikonomopoulou I, Migueles RP, Soneji S, Livigni A, et al. (2008) Anterior definitive endoderm from ESCs reveals a role for FGF signaling. Cell Stem Cell 3: 402–415.
28. Bort R, Martinez-Barbera JP, Beddington RS, Zaret KS (2004) Hex homeobox gene-dependent tissue positioning is required for organogenesis of the ventral pancreas. Development 131: 797–806.

STEM CELLS AND DEVELOPMENT
Volume 23, Number 18, 2014

DOI: 10.1089/scd.2013.0469

Plasma Elevation of Vascular Endothelial Growth Factor Leads to the Reduction of Mouse Hematopoietic and Mesenchymal Stem/Progenitor Cells in the Bone Marrow

Katsuhisa Tashiro,[1,*] Aki Nonaka,[1,2,*] Nobue Hirata,[1] Tomoko Yamaguchi,[1] Hiroyuki Mizuguchi,[3–6] and Kenji Kawabata[1,2]

Vascular endothelial growth factor (VEGF) is reported to exhibit potent hematopoietic stem/progenitor cell (HSPC) mobilization activity. However, the detailed mechanisms of HSPC mobilization by VEGF have not been examined. In this study, we investigated the effect of VEGF on bone marrow (BM) cell and the BM environment by intravenous injection of VEGF-expressing adenovirus vector (Ad-VEGF) into mice. A colony assay using peripheral blood cells revealed that plasma elevation of VEGF leads to the mobilization of HSPCs into the circulation. Granulocyte colony-stimulating factor (G-CSF) is known to mobilize HSPCs by decreasing CXC chemokine ligand 12 (CXCL12) levels in the BM. However, we found almost no changes in the CXCL12 levels in the BM after Ad-VEGF injection, suggesting that VEGF can alter the BM microenvironment by different mechanisms from G-CSF. Furthermore, flow cytometric analysis and colony forming unit-fibroblast assay showed a reduction in the number of mesenchymal progenitor cells (MPCs), which have been reported to serve as niche cells to support HSPCs, in the BM of Ad-VEGF-injected mice. Adhesion of donor cells to the recipient BM after transplantation was also impaired in mice injected with Ad-VEGF, suggesting a decrease in the niche cell number. We also observed a dose-dependent chemoattractive effect of VEGF on primary BM stromal cells in vitro. These data suggest that VEGF alters the distribution of MPCs in the BM and can also mobilize MPCs to peripheral tissues. Taken together, our results imply that VEGF-elicited egress of HSPCs would be mediated, in part, by changing the number of MPCs in the BM.

Introduction

HEMATOPOIETIC STEM CELLS (HSCs) sustain blood production throughout life. In a steady state, HSCs exist within the bone marrow (BM) and remain largely quiescent and self-renew at a low rate to avoid their exhaustion. By contrast, HSCs can actively proliferate, differentiate into progenitor cells, or egress from the BM into the circulation in some situations, such as tissue damage-induced cell death and increased plasma levels of hematopoietic cytokines, including the granulocyte colony-stimulating factor (G-CSF). These dynamic behaviors of HSCs are controlled by a local specific microenvironment called niches [1–8]. The non-hematopoietic cells, such as endosteal osteoblasts and perivascular mesenchymal progenitor cells (MPCs), are reported to function as niche cells by supplying several HSC maintenance factors, including the CXC chemokine ligand 12 (CXCL12). Indeed, previous studies have shown that decreased levels of CXCL12 in the BM caused hematopoietic stem/progenitor cell (HSPC) mobilization, indicating the pivotal role of CXCL12 signaling in HSPC egress [9,10].

Not only is the vascular endothelial growth factor (VEGF) a well-known factor in angiogenesis, but it also plays an important role in the growth and differentiation of hematopoietic cells. Homozygous or heterozygous deletion of VEGF in mice leads to early embryonic lethality because of impaired vascular angiogenesis and hematopoiesis [11,12]. By conditional deletion of VEGF in hematopoietic cells, but not in stromal cells, Ferrara and colleagues clearly showed that VEGF is required for survival and repopulation

[1]Laboratory of Stem Cell Regulation, National Institute of Biomedical Innovation, Osaka, Japan.
Laboratory of [2]Biomedical Innovation and [3]Biochemistry and Molecular Biology, Graduate School of Pharmaceutical Sciences, Osaka University, Osaka, Japan.
[4]iPS Cell-Based Research Project on Hepatic Toxicity and Metabolism, Graduate School of Pharmaceutical Sciences, Osaka University, Osaka, Japan.
[5]Laboratory of Hepatocyte Regulation, National Institute of Biomedical Innovation, Osaka, Japan.
[6]The Center for Advanced Medical Engineering and Informatics, Osaka University, Osaka, Japan.
*These two authors contributed equally to this work.